DSPACE

https://dspace.org/

A chemical, mineralogical and petrographic study of the Koppies bentonite deposits within the Volksrust Formation, South Africa

Kunneke, Luke Karl

2019-07
https://hdl.handle.net/10539/29640

Downloaded from a DSpace repository. https://dspace.org/



A chemical, mineralogical and petrographic study of the Koppies bentonite deposits within the Volksrust Formation, South Africa

Luke Karl Kunneke

761422

A research report submitted to the Faculty of Science, University of the Witwatersrand, Johannesburg, in partial fulfilment of the requirements for the degree of Master of Science.

July 2019

Declaration

I declare that this research report is my own unaided work. It is being submitted in fulfilment of the degree of Master of Science to the University of the Witwatersrand, Johannesburg. It has not been submitted before for any degree or examination to any other university.



Luke Kunneke

761422

Signed on the 29th July 2019 at Johannesburg, South Africa

Abstract

The Koppies bentonite deposits are hosted within the Permian Volksrust Formation, Ecca Group, Karoo Supergroup, deposited in a deep to shallow marine environment, while the locally associated Greenlands Formation represents a deformed remnant of the Vredefort impact (*ca.* 2.02 Ga). Fieldwork suggests that the Greenlands Formation, comprising amphibolites, komatiites, actinolite-chlorite schists, dykes and sills, did not weather *in-situ* (as suggested by some authors) to form bentonite due to the lack of allophane material. It rather served as a palaeo-high, assisting in structural control of the deposits. Low energy mechanisms transported pyroclastic ash into palaeo-low embayments within the Greenlands Formation.

The source and alteration process responsible for the formation of the Koppies bentonite deposits was uncertain, primarily due to ambiguity in analytical results obtained in previous studies. This study aims to elucidate how these deposits were formed and incorporate this understanding into a basic exploration model.

Samples obtained from the Blaauwboschpoort pit, Oceaan pit and overlying shales of the Koppies bentonite deposits underwent mineralogical, geochemical and optical investigation. Mineralogical results suggest that smectite clay accounts for up to 99% of the samples with minor proportions of quartz, mica, chlorite/kaolinite, plagioclase, calcite and K-feldspar. Geochemical analyses suggest a felsic, trachyandesitic ash, derived from an intra-plate granitic/anorogenic setting.

Small concentrations of zircons and apatite were recovered with the majority of zircon grains occurring as euhedral, small, oscillatory zoned and colourless grains, possibly illustrating a singular source. Zircons with minor rounded edges indicated some transport, while a few large, zoned, rounded grains likely reflect external inherited detritus.

A comparison between the geochemical signature of the Koppies bentonites and other known Gondwanan lithologies showed similarities to the Choiyoi Group volcanics located in South America, which is believed to have supplied the ash that lead to the neoformation of the Koppies bentonite. Strong comparative evidence is seen in age (265 – 251 Ma), mineralogy, chemistry and location. The lack of opal-CT within the bentonite also points to a lower thermal gradient between the water and tuffaceous ash, which occurred due to aeolian transport from a distant volcanic event. Aeolian processes involved both high-altitude drift and dominant prevailing tropospheric winds, which kept large quantities of ash particles in suspension over a long distance. The low energy marine environment of the Main Karoo Basin would have

provided favourable conditions for ash to settle out of suspension and deposit on the floor of the laterally extensive basin controlled by palaeo-lows and embayments. The interaction of initial seawater and subsequent meteoric water within the ash resulted in leaching of Si, K and Na, and enrichment of Ca and Mg. Favourable factors for secondary supergene alteration and diagenesis of the felsic ash is evidenced by a strong weathering signature within the chemical index of alteration graph.

A stratigraphic interval within the Volksrust Formation units needs to be defined. The geographic position along current drainage lines, with shallow water tables to promote chemical alteration, is a crucial factor in localised bentonite formation. Such parameters can be considered as integral in further exploration. Older lithologies, which created palaeo-highs with accompanying palaeo-lows acted as a suitable embayment for ash accumulation, alteration and preservation and *in-situ* formation of bentonite.

Acknowledgements

This research was supported by G&W Base and Industrial Minerals (PTY) LTD and I would like to thank them for the opportunity to undertake this endeavour.

The CL images within this paper are part of an on-going investigation into the age of the Koppies bentonite deposit, which is funded by the DST-NRE Centre of Excellence in Palaeoscience (CoE-Pal) and the NRF African Origins Platform (AOP), and I would like to thank Robert Muir and Rose Prevec for permission to include them in this study.

Individual thanks must go to Richard da Silva for his assistance and knowledge-sharing in the conceptualisation and direction of this study, and his guidance especially during the earlier versions of this document. The countless hours spent in discussion helped shape the backbone of this research report.

I am also indebted to my supervisor, Professor Judith Kinnaird for continuously encouraging me to push through my limitations through her meticulously high standard of editorial, geological and scientific knowledge.

My thanks go to Michael-John McCall for spending crucial hours reviewing and providing constructive comments on the later versions of this document. His expertise and guidance have helped shape and refine my vision for the final research report.

Finally, I thank my partner, Chane, for being a solid base of continuous positivity, encouragement, belief, and continued support without which I would not have had the determination to finish this difficult endeavour.

Contents

Declaration....ii

Abstract....iii

Acknowledgements....v

List of Figures....viii

List of Tables, List of Symblols....x

Nomenclature....x

Chapter 1 - Introduction....1

1.1. Background....1

1.2. Study area....2

1.3. Aims and objectives....3

1.4. Hypothesis and existing literature....4

Chapter 2 - Bentonite fundamentals, regional occurrences and contextual geology....5

2.1. Bentonite definitions....5

2.2. Fundamental mechanisms of bentonite formation....5

2.2.1. Thermal driven alteration....7

2.2.2. Supergene leaching....9

2.3. South African bentonite deposits....9

2.4. Geological setting of the Main Karoo Basin and Greenlands Formation....10

2.5. Local Geology of the Greenlands Formation and surrounding Koppies bentonite deposits....12

2.6. Closing comment....16

Chapter 3 - Methodology and analytical techniques....17

3.1. Introduction....17

3.2. Sample recovery....17

3.3. Physical investigation....20

3.4 Sample preparation and analysis....20

3.4.1. X-ray Diffraction (XRD)....20

3.4.2. X-ray Fluorescence (XRF) 20
3.4.3. Scanning Electron Microscopy (SEM) 21
3.4.4. Heavy Mineral Separation and Cathodoluminescence (CL) 21
Chapter 4 - Results 22
4.1. Physical investigation and field observations 22
4.2. Petrographic observations 26
4.2.1 SEM 26
4.2.2. Heavy mineral recovery and cathodoluminescence 27
4.3. Data Presentation 29
4.3.1. Geochemical results for major and trace elements 29
4.3.2. Mineralogy of the Blaauwboschpoort and overlying shales 29
4.4. Closing comment 32
Chapter 5 - Interpretation 33
5.1. Relationship between the Koppies bentonite and Greenlands Formation 33
5.2. Geochemical perspectives 33
5.3. Environment 34
5.4. Weathering 36
5.5. Provenance 37
5.6. Optical interpretations 39
Chapter 6 - Discussion: Formation of the Koppies bentonite deposits 40
6.1. Permian ash deposits 40
6.2. Source 40
6.3. Transport and deposition 42
6.4. Alteration 43
6.5. Implications for exploration 44
Chapter 7 - Conclusion 45
References 47

List of Figures

Figure 1: Mining and beneficiation to principal market application flow diagram for bentonites. Note that most deposits are free-dig and do not require drill and blast techniques (Grim and Guven, 1978). 2

Figure 2: Study area of the Koppies bentonite deposits. The mining right boundary (in red) is situated between the N1 and R82 national roads in the Free State, Blaauwboschpoort pit (south), Oceaan rehabilitated pit (north) 3

Figure 3: Chemical weathering flow diagram of minerals within the glass constituent of volcanic ash. Smectite illustrated in orange is formed by the progressive breakdown of amphibole, biotite, plagioclase and pyroxene (Dill, 2010)..... 8

Figure 4: Geological map illustrating various upturned sequences in the Vredefort Dome and Greenlands Formation (circled in red) (Lana *et al*., 2003). 13

Figure 5:Geological map of the Greenlands Formation. The dotted lines represent the farm boundaries, while the wavy lineaments represent the trend of the Broodkop shear zone. The red circles illustrate the bentonite deposits located on the farm Blaauwboschpoort and Oceaan (Lana *et al*., 2003). 15

Figure 6: Sample locality map for the samples 1-19 taken from the *Blaauwboschpoort* and Oceaan deposits and surrounding sub-pits. 19

Figure 7: Composite geological map of the Greenlands Formation with the location of various bentonite deposits and occurrences 23

Figure 8: Stratigraphy and field evidence of the Koppies bentonite deposits. (a) Stratigraphic column, (b) *In-situ* khaki brown to grey bentonite seam identified as sample 2, the darker colour is due to characteristic water retention in comparison to overlying micaceous shales, (c) Structureless, and waxy orange bentonite near Sample 6 illustrating the colloidal nature. Notable manganese growths are evident. 24

Figure 9: Field evidence and various inclusions within the Koppies bentonite deposit. a) Sample 7 showing boxwork quartz precipitate found within shallow extent of bentonite orebody. b) Dendritic manganese oxide growth in cracks within khaki brown bentonite at Sample 5 locality. c) Irregularly shaped, large barium-rich siderite concretion formed within the bentonite at Sample 4 locality. d) Bentonite present on outer surface of siderite concretion. 25

Figure 10: Scanning electron photomicrographs of smectite textures observed in the Blaauwboschpoort bentonite. (a) Smectite dominated matrix illustrating crenulated

edges of the flakes. (b) Booklet, face to face associations of smectite flakes (circled in white). 26

Figure 11: Scanning electron photomicrographs of inclusion minerals within the smectite matrix observed in the Blaauwboschpoort bentonite. (a) Void in the smectite matrix illustrating a remnant rounded quartz crystal (circled in white), (b) Individual zeolite grain amongst smectite mass (circled in white) 27

Figure 12: Scanning electron photomicrographs of the boxwork quartz and bentonite contact within a pre-existing crack within the Blaauwboschpoort bentonite deposit (a) Sharp contact between the quartz precipitate and bentonite (annotated in white), (b) Zoomed-in angular quartz crystals with smectite surface coatings. 27

Figure 13: Recovered grains of fragmented, elongated, stumpy, large, small and zoned heavy minerals from the Blaauwboschpoort bentonite. White circles illustrate the zircons while the remainder of crystals represent apatite grains (87x magnification). (a) Zoned euhedral zircon crystals. (b) Fragmented, rounded zircon crystals. 28

Figure 14: Immobile element Al versus mobile/immobile elements for the Koppies bentonite deposits and overlying Volksrust shales. Trend lines illustrate enrichment as a negative intercept and depletion as a positive intercept for a given element (Christidis, 1998). 35

Figure 15: Ternary plot of dominant cations present in the Koppies bentonite in relation to the overlying shales (atypical chemistry of shales). The Koppies bentonite samples reflect a Na depleted array, similar to the Wyoming bentonite deposits (Altaner *et al.*, 1984, Knechtel and Patterson, 1962). 36

Figure 16: Ternary diagram of A-CN-K, where A = Al_2O_3, C = CaO N =Na_2O, K =K_2O (Nesbitt and Young, 1984). Bentonite plots in strong weathering field while overlying shales plot between the intermediate and weak weathering fields. 37

Figure 17: Bivariate trace element plots for the Blaauwboschpoort bentonite deposit. (a) Rhyolitic character versus alkalinity graph (Winchester and Floyd, 1977). (b) Discrimination diagram of Nb vs. Y (Pearce *et al.*, 1984) 38

Figure 18: Simplified palaeo geological map illustrating the approximate distance between the Choiyoi Group and Volksrust Formation which is contained in the NW section of the Ecca Group (McKay *et al.*, 2016). 42

Figure 19: Idealised sketch of the depositional setting and the structural relationship between the Koppies bentonite and Greenlands Formation. 43

List of Tables

Table 1: Details and variables for the multiple stages responsible for bentonite formation (, Cabellero *et al*., 1991, Christidis, 2001, Galan, 2006, Gardam *et al*., 2009, Grim and Guven, 1978, Elzea and Murray, 1990, Slaughter and Hamil, 2013)..... 6

Table 2: Bentonite occurrences and deposits in South Africa (youngest to oldest) (Horn and Strydom, 1998, Bordy and Abrahams, 2016, Manninen *et al*., 2008, Schmidt, 1976) 11

Table 3: Synopsis of samples obtained, including associated analytical methods employed18

Table 4: Quantitative major geochemical results of the Blaauwboschpoort and Oceaan bentonite and overlying shale samples 30

Table 5: Quantitative selected trace geochemical results of bentonite from the Blaauwboschpoort deposit..... 31

Table 6: Semi-quantitative mineralogical data of the Blaauwboschpoort bentonite, overlying shale and topsoil..... 32

List of Symbols

Ga – Billion years

Ma – Million years

Mbs – Metres below surface

Ppm – Parts per million

Nomenclature

CEC – cation exchange capacity

CIA – chemical index of alteration

Free-dig – ability to mine in open cast manner without the need to blast

LOI – loss on ignition defined as a percentage loss of fluids during drying stage

MKB – Main Karoo Basin

Opal-CT – Opal cristobalite tridymite

Plinian style eruption – Large, violent volcanic eruption producing large volumes of pyroclastic ash

Chapter 1

Introduction

1.1. Background

Bentonite represents a widely used and significant industrial mineral in a global context. The demand and application of bentonite, particularly in an ever-changing market and volatile economy, is notably consistent (Scogings, 2016). Key physiognomies of bentonite such as thixotropy, ductility, adsorption and cation exchange capacity define its applicability in industrial applications (Figure 1). These applications range from traditional metal casting, pelletisation in chrome beneficiation, drilling clay and adsorption agents, whilst research into niche markets such as nano-technological materials and medicine are ongoing (Gong *et al*., 2016).

The crystal structure of bentonite is a hydrous phyllosilicate that comprises flat platelets and a high surface area (Enslin *et al*., 2010). The octahedral layer within the crystal structure can absorb and retain cations and anions in an exchangeable state as a result of electrostatic forces which act on the surface of particles (Heckroodt, 1991). In this regard the most reactive interlayer cation, Na^{+}, is most sought after based on its high swelling capabilities while less reactive Ca^{2+}, Mg^{2+}, K^{+}, and Li^{+} bentonites are commonly mined but require further beneficiation. During beneficiation, the inferior bentonites are dosed with sodium carbonate to supplement the bentonite by replacing various less reactive cations with Na^{+} (Dill, 2010). Variable amounts of inert minerals such as opaline silica, kaolinite, illite, feldspar, quartz, zeolite and gypsum can also be present but with subsequent grinding, calcination and treatment with organic compounds these impurities can be removed (Grim, 1972).

Market share, production and export of bentonite is dominated by the USA, China, India and Greece, while countries with smaller reserves mine bentonite on a “subsistence” or domestic scale (Grim and Guven, 1978). One of two current producers of bentonite within South Africa - G&W Base and Industrial Minerals - mines the Blaauwboschpoort bentonite deposit, often referred to as the Koppies bentonite deposits (Scogings, 2016).

Limited published research exists on the various small-scale deposits within the Koppies bentonite fields (Horn & Strydom, 1998). In this regard, much preceding work has focused solely on specific characteristics of the bentonite as opposed to a holistic, scientific overview and characterisation. Therefore, the utilisation and amalgamation of a diverse set of analytical methods is essential in the characterisation and comprehension of the Koppies bentonite deposits.

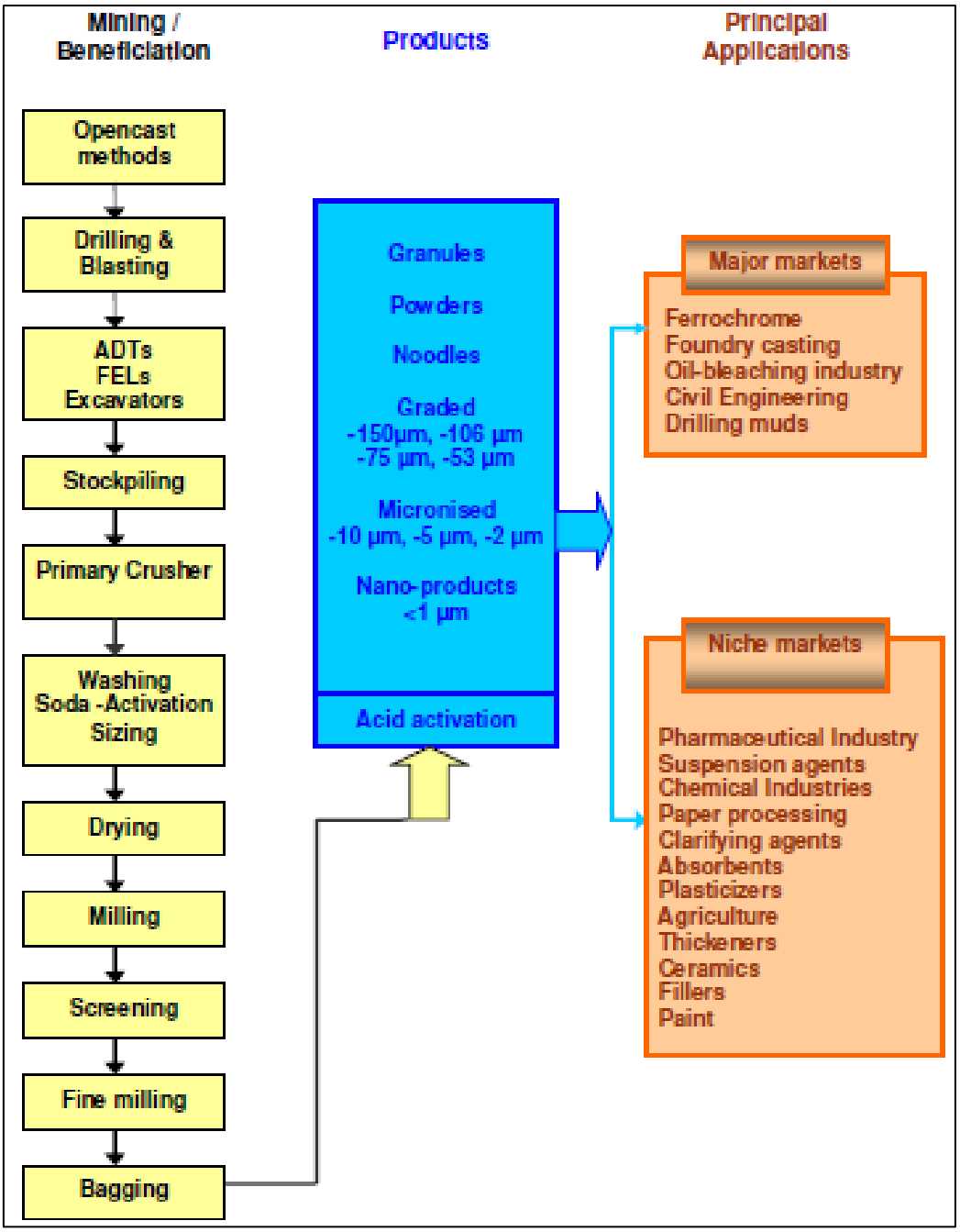


Figure 1: Mining and beneficiation to principal market application flow diagram for bentonites. Note that most deposits are free-dig and do not require drill and blast techniques (From: Grim and Guven, 1978).

1.2. Study area

The study area is focused on a group of bentonite deposits located 12 km north of the town of Koppies, Ngwathe Local Municipality in the Free State Province of South Africa. Multiple small-scale deposits exist around the Greenlands Formation, deformed by the Vredefort impact event about 2.2 billion years ago (Lana *et al*., 2003). The two main deposits are known as the Oceaan and Blaauwboschpoort orebodies (Figure 2), with smaller occurrences scattered throughout the immediate area. Mining of the Oceaan deposit ceased in 2008, while the

Blaauwboschpoort sub-pits are actively strip-mined during the winter months of the year, with concurrent rehabilitation of the mined-out areas.

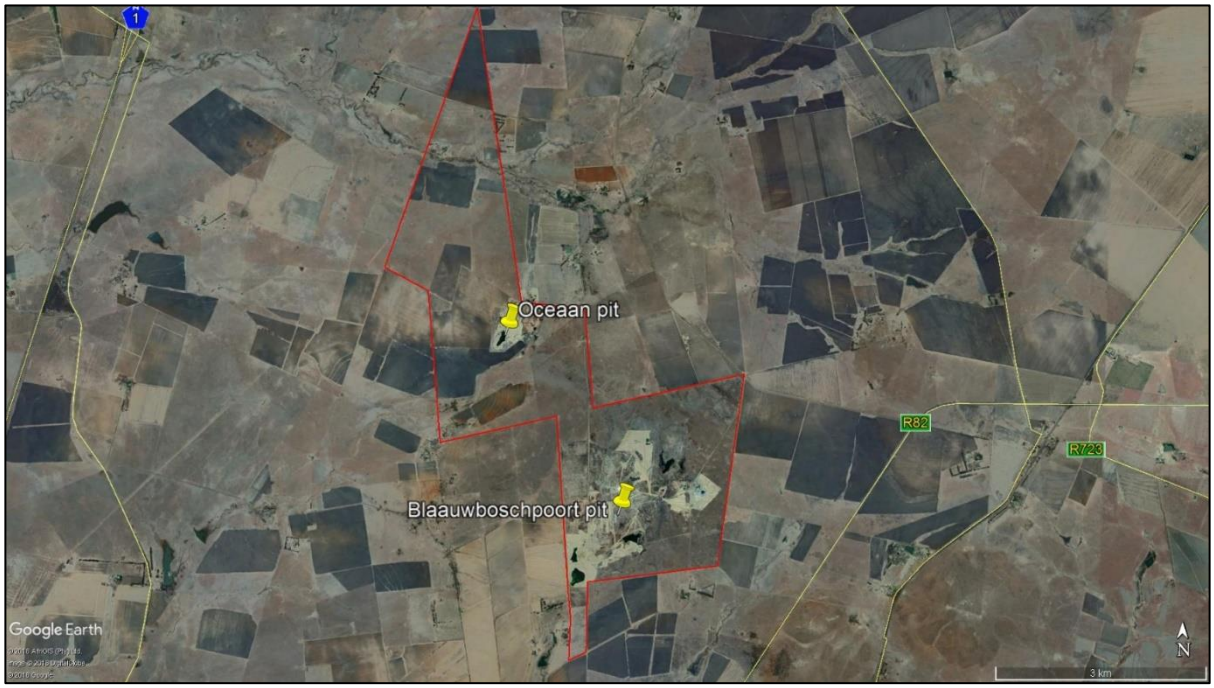


Figure 2: Study area of the Koppies bentonite deposits. The mining right boundary (in red) is situated between the N1 and R82 national roads in the Free State, Blaauwboschpoort pit (south), Oceaan rehabilitated pit (north).

1.3. Aims and objectives

The aim of this research is to analytically define the source and processes responsible for the formation of the Koppies bentonite deposit. The objectives of this study are two-fold, namely: (1) to aid in future detailed target generation to minimise capital expenditure for G&W Base and Industrial Minerals, and (2) to provide publicly-available analytical results and evidence for use in future research. Accordingly, the scope of the study is as follows:

- Orebody delineation in relation to surrounding geology, with a focus on field relationships, contacts, terminations and structures;
- Identification of the explicit processes which acted on the Koppies bentonite through physical, mineralogical and chemical examination of trends;
- Petrography of the bentonite by means of the scanning electron microscope (SEM) with a particular focus paid to the presence/absence of volcanic remnant structures and minerals;
- Isolated heavy minerals, mainly zircon, analysed via cathodoluminescence (CL), with attention to zircon morphology. The zircon CL images are part of another ongoing study and have been included within this study with permission. See acknowledgements for details.

1.4. Hypothesis and existing literature

This study explores the two main questions listed in 1.4(i) and 1.4(ii) below and seeks to challenge the conclusions of previous authors in relation to those questions on the basis of new chemistry, field observations and optical analyses, namely:

i. Is the source material from which the Koppies bentonite deposit formed of volcanoclastic ash origin or a result of in-situ chemical weathering of basic or acidic rocks within the Greenlands Formation?
   - According to Coetzee & Hanekom (1966), deposition in an alkaline basin led to dissolution-precipitation of bentonite rather than alteration of a hypothetical tuff.
   - Grim & Guven (1978) suggest that lack of relict structures or non-smectite minerals indicates a volcanic ash parent, although they give no evidence of a source to substantiate volcanic activity.
   - Heckroodt (1991) supported *in-situ* alteration of a layered volcanic tuff for the origin of the bentonite citing the lack of quartz in the Koppies bentonite.
   - Horn & Strydom (1998) incorporated petrographic work to illustrate a volcanic ash fabric within larger glass-shard morphologies of the bentonite.

ii. What type of geological setting dominated and favoured the formation of the Koppies bentonite deposits?
   - The pH of the bentonite ranges from 8.2 - 9 (Horn & Strydom, 1998).
   - The alteration was in a shallow brackish water environment (Horn & Strydom, 1998).
   - The bentonite developed in palaeo-topographic lows within the intra-Karoo stratigraphy (Minnitt & Reimold, 2000).

The subsequent chapter aims to build a foundation of bentonite principles and site-specific geology onto which this research report builds.

Chapter 2

Bentonite fundamentals, regional occurrences and contextual geology

This chapter introduces the reader to definitions of and associated mechanisms for the formation of bentonite. Macro- to meso-scale observations provide both a regional and local context of bentonites in general, whilst meso- to micro-scale geology attempts to establish a detailed, site-specific characterisation of the Koppies bentonite deposits.

2.1. Bentonite definitions

Bentonite was initially defined as "*a rock composed essentially of a crystalline clay-like mineral formed by devitrification and chemical alteration of a glassy igneous material, usually a tuff or volcanic ash*" (Ross and Shannon, 1926). This definition was amended by Grim (1972), to a "*clay consisting of smectite group minerals, regardless of occurrence or origin*". This allowed for bentonites derived from sedimentary and hydrothermal (argillisation) (Christidis *et al*., 1995) sources to be included alongside volcanic-derived clay (Bazargani-Guilani *et al*., 2008). Currently, bentonite is defined as a clay consisting predominantly of a specific di-octahedral smectite mineral known as montmorillonite and acknowledged as an alteration product formed during the weathering of a parent rock (Christidis and Huff, 2009).

Notable discrepancies exist in the literature regarding the definition and classification of the Koppies clay. While most authors refer to the clay as bentonite, additional nomenclature has been established e.g. '*Fullers earth clay'* and '*bleaching clay'.* These terms should however only be used to infer the collective presence of minerals such as smectite, kaolinite and attapulgite. For the purpose of this research, the author will refer to the Koppies clay as bentonite (*sensu stricto)*.

2.2. Fundamental mechanisms of bentonite formation

The process responsible for bentonite formation is not a binary reaction but rather a multi-stage, multi-variable alteration reaction (Caballero *et al*., 1991). These variables act to alter an otherwise linear prograde reaction to highly site-specific conditions (Christidis, 2008). Therefore, an understanding of a separate classification scheme, namely the eruptive, transport and alteration phases is essential to comprehend both the active and passive reactions responsible for the formation of bentonite in general (Table 1).

Table 1: Details and variables for the multiple stages responsible for bentonite formation (Cabellero *et al*., 1991, Christidis, 2001, Galan, 2006, Gardam *et al*., 2009, Grim and Guven, 1978, Elzea and Murray, 1990, Slaughter and Hamil, 2013).

Phase	Detail	Variables
Eruption phase	The initial eruptive phase refers to the volcanic event which forms the precursor material that later weathers to bentonite. Compositionally the material can range between volcanic pyroclastic ash, plutonic or volcanic rocks. For the majority of bentonite deposits this material can usually be traced to a violent Plinian-type event, while in other instances older in situ igneous source rocks act as a weathered source.	• Style of eruption • Tectonic setting • Composition of precursor rock • Size of ash particles/glass shards
Transport/ deposition phase	The transport and deposition phase applies to primary tuffaceous material or secondary physically weathered and remobilised volcanic source rocks. Processes act to transport weathered material via high-energy airborne and fluvial mechanisms to low energy depositional environments. At the point of contact between the hot bentonite and cold water the subsequent alteration phase initiates. Preferable settings for deposition and accumulation of the ash are within sedimentary basins and or deltaic settings, where fine ash particles can deposit out of suspension and accumulate.	• Prevalent winds and fluvial currents • Depositional environment • Chemistry of interacting water • Thermal contrast of fluid and ash • Distance from eruption to deposition
Alteration phase	The alteration phase is considered most complex due to the number of variables which influence the neoformed site-specific bentonite. Hydrothermal, diagenetic and chemical deuteric alterations of pyroclastic, tuffaceous or volcanic rocks are the primary mechanisms of alteration and bentonite formation.	• pH/Eh conditions • Si and alkali activity • Thermal contrast between ash and water • Abundance of Mg in saline basin • Composition and amount of basin/ meteoric and aqueous fluids • Degree of alteration via diagenesis or supergene leaching

The above phases can be broadly categorised into structural controls which are active prior to the alteration/formation stage and are responsible for the shape, continuity, orientation and location of the deposit (Berry, 1999), while geochemical controls influence the final chemistry of the clay. This is due to parent rock composition; chemistry of basinal/meteoric/aqueous waters (alkalinity); nature of the fluid flow and other secondary processes responsible for element re-mobilisation (Al-Ani and Sarapaa, 2008).

2.2.1. Thermal driven alteration

The quality of bentonite is largely driven by the endothermic reaction that the precursor ash undergoes. Typically, hot pyroclastic ash mingles with cold saline water to form a well-developed bentonite deposit (Christidis and Huff, 2009). High quality bentonite deposits are created through low-medium thermal contrasts, while lower quality deposits, containing silica rich polymorphs such as opal-cristobalite tridymite (opal-CT), are formed through high thermal gradients (Henderson *et al*., 1971).

The glass constituent within volcanic ash serves as a necessary requirement for the initiation of the alteration reaction. The progressive multi-stage chemical weathering reaction is best detailed by Viljoen (1994), and Bordy and Abrahams (2016) who suggest that the interaction of silicic volcanic glass and water/fluid leads to the formation of montmorillonite/smectite, silicification and ions leaching from the clay (Arslan *et al*., 2010). The stable, low temperature mineral, smectite, is favoured in the early stages of this reaction (Galan, 2006, Grim and Guven, 1978).

Favourable minerals (within the glass) for bentonite formation can be sourced from a compositional range between dacitic to rhyolitic vitreous ash (Murray, 2007). Associated minerals contained within the volcanic ash are plagioclase, biotite, amphibole and pyroxene which have the potential to undergo drastic changes in mineralogy (Figure 3). The maturity and quality of the bentonite is dependent on influences from secondary physical and chemical weathering processes, whilst more severe, pervasive alteration can lead to the formation of a mixed clay layer at the expense of smectite (Dill, 2017).

The most common process is the dissolution-precipitation thermal interaction between the ash and saline water; however, various sources of heat can drive the alteration reaction. Diagenetic-derived bentonites are formed by the alteration of existing volcanics in conjunction with alkaline groundwater under diagenetic conditions (Dill, 2010). The increased temperatures and pressures of burial provide the thermal energy responsible for devitrification and ionic diffusion in the volcanics which result in bentonite rich layers that grade into smectite-rich shales (Goldich, 1938). This essentially restricts bentonite deposits to sedimentary packages with thicknesses of less than 4 km as an increased depth of burial results in crystal

lattice disintegration and formation of a variety of phases including cristobalite (Huff *et al*., 1998). In this regard high smectite content is usually indicative of a genetic history with low burial temperatures, usually less than 300 ºC (Al-Ani and Sarapaa, 2008).

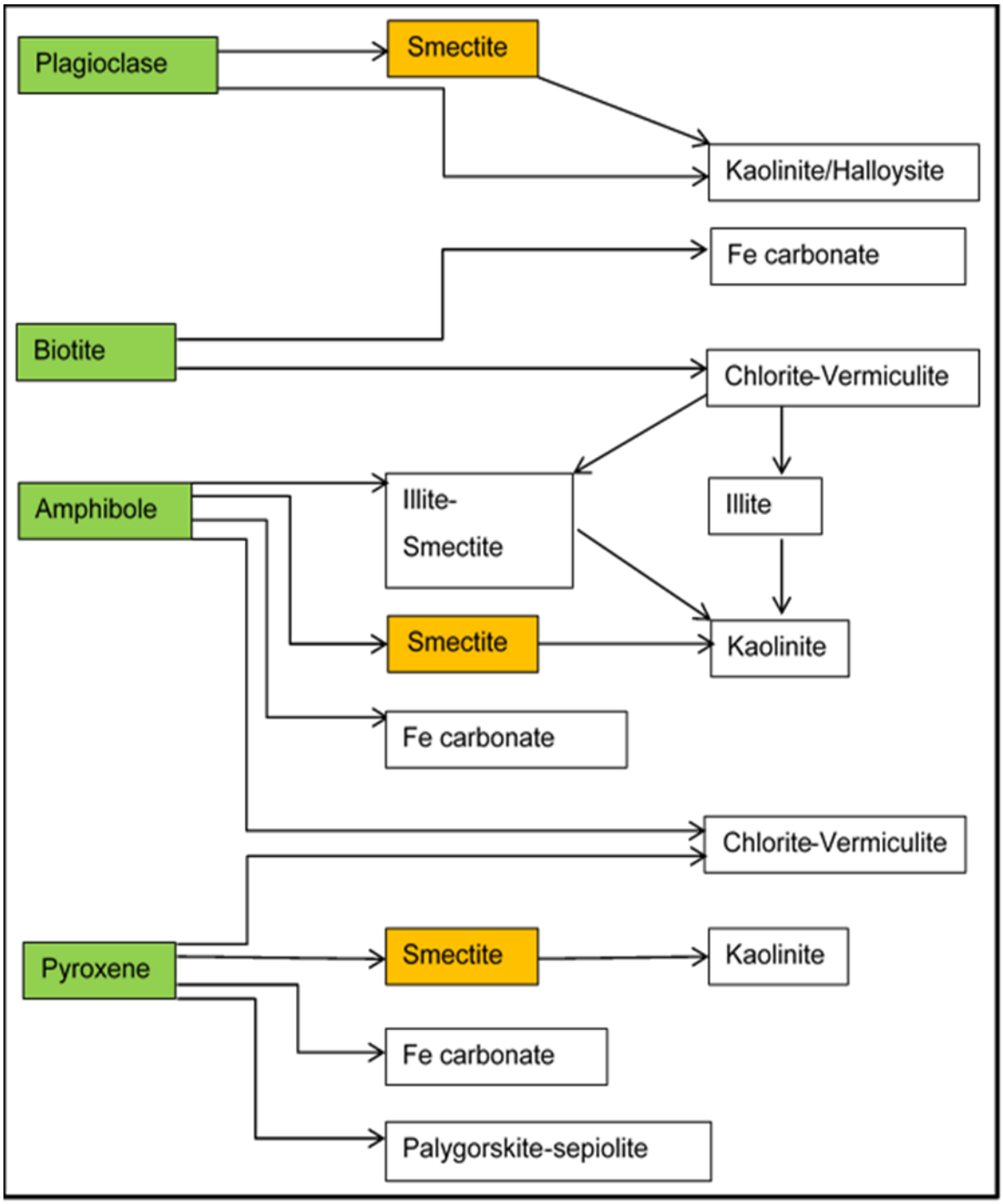


Figure 3: Chemical weathering flow diagram of minerals within the glass constituent of volcanic ash. Smectite illustrated in orange is formed by the progressive breakdown of amphibole, biotite, plagioclase and pyroxene (From: Dill, 2010).

The introduction of hydrothermal fluids containing volatiles into surrounding volcanic rocks also favours bentonite formation through argillisation whereby thermal energy is derived from ingressing fluids (Chritidis, 2001). The alteration of Ca-plagioclase or K-feldspar can produce smectite in combination with kaolinite in irregularly shaped deposits which grade into the parent rock through partly altered saprolitic zones (Dill, 2017).

2.2.2. Supergene leaching

Supergene leaching contrasts thermally favoured reactions as it is driven by chemical weathering and oxidation (Grim and Guven, 1978). Alternating wet and dry conditions promote silica and alkali elements to mobilise and leach from the volcanic ash (Galan, 2006). The result is di-octahedral montmorillonites such as smectite and/or beidellite which are enriched in iron (Dill, 2010). Alteration is restricted to *in-situ* acidic and basic parent rocks containing sufficient calcium and magnesium. Additional factors include environments with high pH, an abundance of basic cations, low lying topography, high silica activity, poor drainage and Mediterranean climates with a well-defined seasonal contrast (Galan, 2006).

2.3. South African bentonite deposits

Bentonite deposits occur globally, with the well-known Wyoming (USA) deposits comprising the world's largest and richest resource (Thorson, 1997, Scogings, 2016, Elzea and Murray, 1990). In a South African context multiple tuffaceous and bentonitic layers exist within the Karoo basin of South Africa while deposits of relatively pure bentonite are restricted to the Koppies district in the Free State and Heidelberg/Plettenberg Bay districts of the Western Cape. A relatively impure bentonite deposit also occurs in the Mkuze district of KwaZulu-Natal, while various uneconomic, scattered deposits occur throughout South Africa (Horn and Strydom, 1998). These are further detailed below and in Table 1:

- Quaternary montmorillonite and attapulgite mixed deposits are located inland and are localised over basic rocks such as the Karoo basalts and rocks of the Bushveld igneous complex. These "dirty", mixed, uneconomic clay layer deposits are a result of a weathering profile consistent with soil forming processes (Horn and Strydom, 1998).
- The Western/Eastern Cape Mesozoic Uitenhage Group basins contain conglomeratic beds (Enon Formation), sandstone, siltstone, shale and various ash falls and lavas of the Kirkwood Formation. The bentonite, zeolite and interlayered tuff horizons are controlled by a 600 km long line of half grabens and several Mesozoic rift-related basins (Horn and Strydom, 1998). These Cretaceous bentonite deposits formed as a result of volcanism related to the break-up of Gondwana – a period of massive volcanism worldwide. Bentonite formed as a succession of lenticular-shaped deposits

that are intercalated with sandstone. The lacustrine-derived bentonite-bearing beds are often reworked tuffs and predominantly comprise cristobalite and quartz with an overlying soft siliceous sandstone layer (Horn and Strydom, 1998).

- The Zululand (KwaZulu-Natal) deposit is related to the rhyolitic and basaltic rocks of the Jozini Formation, Lebombo Group of the Karoo Supergroup (Heckroodt, 1991). The Jurassic-aged rhyolitic belts weather through an *in-situ* devitrification process to glassy perlite. Older portions have experienced further deuteric action altering perlite and perlitic pillow lavas to patchy bentonite.
- The Pronksberg deposit is a thin bentonite seam hosted by mudstones and sandstones within the Elliot Formation, Karoo Supergroup. The bentonite (1-2 m thick) is underlain by a characteristic yellow sandstone and overlain by a silicified cherty rock (formerly red mudstone). The deposit formed through the devitrification of felsic volcanic ash which was later reworked and chemically weathered (Bordy and Abrahams, 2016).
- The Oceaan 64 and Blaauwboschpoort 13 deposits, developed within the Volksrust Formation of the Ecca Group, Karoo Supergroup, have been mined since the 1950s. They contain low proportions of impurities, with a predominant smectite mineralogy. These deposits typically contain 20-30% moisture with a pH between 8.2 and 9. The exchangeable cations are Ca^{2+} and Mg^{2+} and chemically resemble the large, well-known Wyoming (USA) deposits (Horn and Strydom, 1998).
- Bentonite associated with coal seams (Vryheid Formation, Karoo Supergroup) at the Vierfontein colliery is overlain by an aeolian sequence. The bentonite has developed in the hanging wall of the uppermost coal horizon while the footwall comprises a calcareous sandstone. Silicification notably increases with increasing depth. The depositional environment of the bentonite is believed to be an estuarine or lagoonal setting (Schmidt, 1976).

2.4. Geological setting of the Main Karoo Basin and Greenlands Formation

The Vredefort meteorite impact occurred at 2.02 Ga and resulted in the upheaval of surrounding rocks (Reimold and Gibson, 1996). Metasedimentary rocks from the Dominion Group, Witwatersrand, Transvaal, Ventersdorp supergroups and the Archean basement were affected (Slawson, 1976). The metamorphic grades of the exposed rocks range from granulite facies in the core of the impact to amphibolite facies in the surrounding areas (Lana *et al*., 2003). Following the impact, the "*amalgamation of continental plates led to the formation of the supercontinent Gondwana on which extensive intracratonic basins developed*" (Hunter *et al*., 2006) of which the Main Karoo Basin (MKB) in South Africa is one - regarded as the largest basin in southern Africa by lateral extent (Geel *et al*., 2013).

Table 2: Bentonite occurrences and deposits in South Africa (youngest to oldest) (Horn and Strydom, 1998, Bordy and Abrahams, 2016, Manninen *et al*., 2008, Schmidt, 1976)

Age	Bentonite deposits	Location	Source of ash and comments
Variable	Palygorskite, montmorillonite, sepiolite mixed horizons	Dwaalboom, Northam, Crecy, Immerpan, Burgersfort, Platreef, Naboomspruit, Hotazel (Northern Cape, Limpopo)	Localised over basic rocks, Karoo basalts or BIC, high seasonal rainfall (inferior not mined)
145-66 Ma	Cretaceous bentonite deposits	Uitenhage, Plettenberg Bay, Knysna, Oudtsoorn, Heidelberg, Swellendam, Port Elizabeth (Western and Eastern Cape)	Kirkwood Volcanics
180 Ma	Jurassic-aged bentonite and perlite deposits	Mkuzi (KwaZulu-Natal)	Basaltic to acidic volcanic complexes associated with Lebombo Volcanics
200-174 Ma	Early Jurassic bentonite deposit	Pronksberg (Eastern Cape)	1 metre thick deposit (Elliot Formation), felsic composition possibly related to southwest Gondwana
260-252 Ma (based on stratigraphic constraints of the enclosing Volksrust Formation)	Late Permian (based on stratigraphic constraints of the enclosing Volksrust Formation) bentonite deposits	Koppies (Free State)	Contrasting models exist
270-260 Ma	Middle Permian bentonite deposit	Groenfontein (Free State)	Associated with coal seams

The MKB developed through northward subduction of oceanic lithosphere (Catuneanu *et al.,* 2005); and is constrained behind a magmatic arc and Cape Fold Belt near the southern coast of South Africa (Catuneanu *et al*., 1998). The MKB is unique in tectonic setting as it is defined as a retro-arc foreland basin contrary to surrounding Karoo basins which signify intracratonic sag or rift basins (Johnson *et al*., 1996). The complexity of the MKB as a whole is related to its mode of origin, being that of a reducing marine, lacustrine, deltaic and fluvial deep and shallow water marine turbiditic environment which resulted in sequences up to thousands of metres thick (Johnson *et al*., 2006). The MKB grades from shallow marine in the north to deeper marine in the southern extent (Smith *et al*., 1993).

Located in the southeast of the Vredefort impact structure and in the northwest of the broader MKB, is an upturned Swazian aged greenstone outlier (Figure 4). Originally the outlier was defined as the Greenlands Greenstone Complex (Minnitt *et al*., 1994); however, later renamed as the Greenlands Formation by the South African Council for Stratigraphy (Minnitt and Reimold, 2000).

The Late Carboniferous to Early Jurassic MKB hosts large, strike-extensive reserves of coal and on a more localised scale, bentonite deposits (Minnitt *et al*., 1994). The bentonite deposits of focus are located within the Volksrust Formation within the MKB surrounding the Greenlands Formation.

2.5. Local Geology of the Greenlands Formation and surrounding Koppies bentonite deposits

The Greenlands Formation was believed to have acted on a localised scale as a weather resistant palaeo-high during the deposition of the Palaeozoic to Mesozoic Karoo Supergroup (Minnitt and Reimold, 2000). The shales from the Volksrust Formation within the Ecca Group of the Karoo Supergroup act as a veneer, obscuring the edges and deeper extent of the present day Greenlands Formation.

Komatiite and komatiitic basaltic compositions dominate the Greenlands Formation (Figure 5). The volcanic origin for the sequence is evidenced by pillow structures, flow banding and spinifex textures in the lower metamorphosed zones in the south eastern flank of the exposed formation on Hattingsrust 68 and a portion of Blaauwboschpoort 13 (Minnitt *et al*., 1994). Mid-greenschist facies metamorphism has, however, altered the rocks into a sequence of mafic to ultramafic chlorite-actinolite schists enclosing lenses of quartz-sericite-biotite with a northwest trending schistosity (Lana *et al*., 2003).

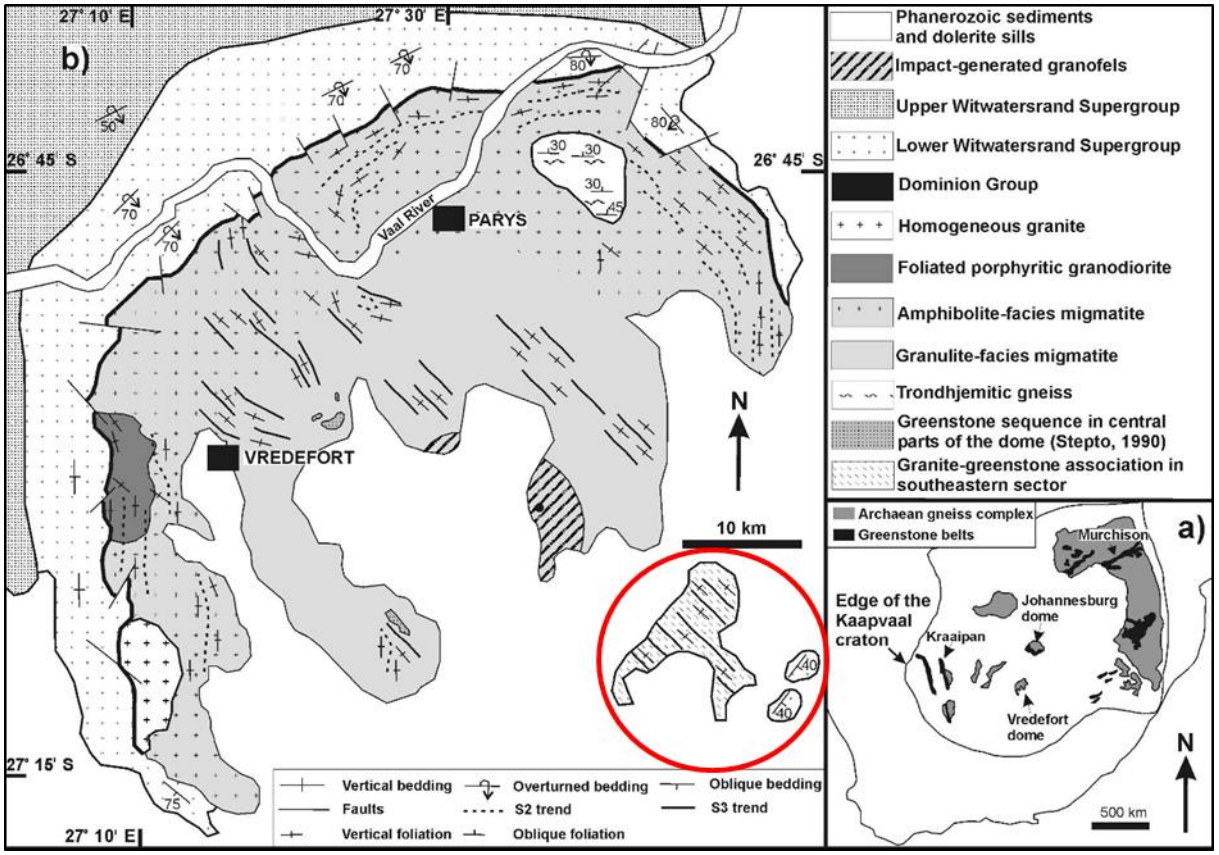


Figure 4: Geological map illustrating various upturned sequences in the Vredefort Dome and Greenlands Formation (circled in red) (From: Lana *et al*., 2003).

To the northwest of the Greenlands Formation, the Broodkop Shear Zone (orientation evidenced by the S4 fabric) represents a kilometre-wide northeast-southwest dip slip shear zone which includes high grade amphibolites and migmatitic trondhjemitic gneisses (Lana *et al*., 2006). These foliated amphibolites contain various small lithium-rich spodumene pegmatites, whilst minor feldspar-quartz porphyry and banded iron formations outcrop (Minnitt *et al*., 1994). Tholeiitic compositions and vesicle structures of the amphibolites are indicative of a volcanic precursor (Lana *et al*., 2006).

Pre-impact mafic intrusions have been cross-cut by pseudotachylitic breccia (Minnitt *et al*., 1994). These tholeiitic intrusions contain varied textures and outcrop on farms Goedgunst 315, Avondale 112, Blaauwboschpoort 13, and Hattingsrust 68. A large, post metamorphic gabbroic intrusion exists on Broodkop 304, Ocean 99, and Van der Merwes Dam 37 (Reimold *et al*., 2000). Multiple Karoo-aged (180 Ma) dolerite dykes dominate the remaining area (Reimold *et al*., 2000).

The surrounding Volksrust Formation is stratigraphically confined between the overlying Beaufort Group and underlying Vryheid Formation (Ecca Group) (Johnson *et al*., 2006). The sedimentary package comprises of dark grey-green to black siltstones, mudstones, shales and sandstone lenses, while convolute bedding and ripple lamination occur sporadically

(Johnson *et al*., 2006). The Volksrust Formation represents a coarsening-upwards sequence, which was formed in a deep water basinal to shallow lagoonal coastal embayment environment (Johnson *et al.*, 2006). This 300-metre sequence contains cyclic units between 30-50 metres in thickness (Hancox and Gotz, 2014). Sideritic, phosphatic, carbonate beds (0.75m thick) and concretions (1.5m diameter) are common in the Volksrust Formation, while bentonite deposits are interlayered within the micaceous shales (Schmidt, 1976).

The bentonite is situated within embayments on Blaauwboschpoort 13 and Oceaan 99 around the Greenstone Formation (Figure 5). Referred to collectively as the Koppies bentonite deposits, the orebodies resemble a localised minor scale coal style of mineralisation in that the seams of bentonite are flat lying to lenticular/tabular shaped (Coetzee and Hanekom, 1966). The bentonite ranges in colour from yellowish grey to olive brown, contains 20-30% moisture and is dominated by Ca^{2+} and Mg^{2+} in the octahedral layers. A waxy texture dominates fresh samples while a popcorn texture is prevalent in weathered outcrops (Horn and Strydom, 1998). The contact between the overlying and underlying shales and bentonite seam is a sharp one with a defined visual contrast (Coetzee and Hanekom, 1966). Grim and Guven (1978) noted that the underlying and overlying units are typical Volksrust shales and mudstones with no silicification present (Grim and Guven, 1978).

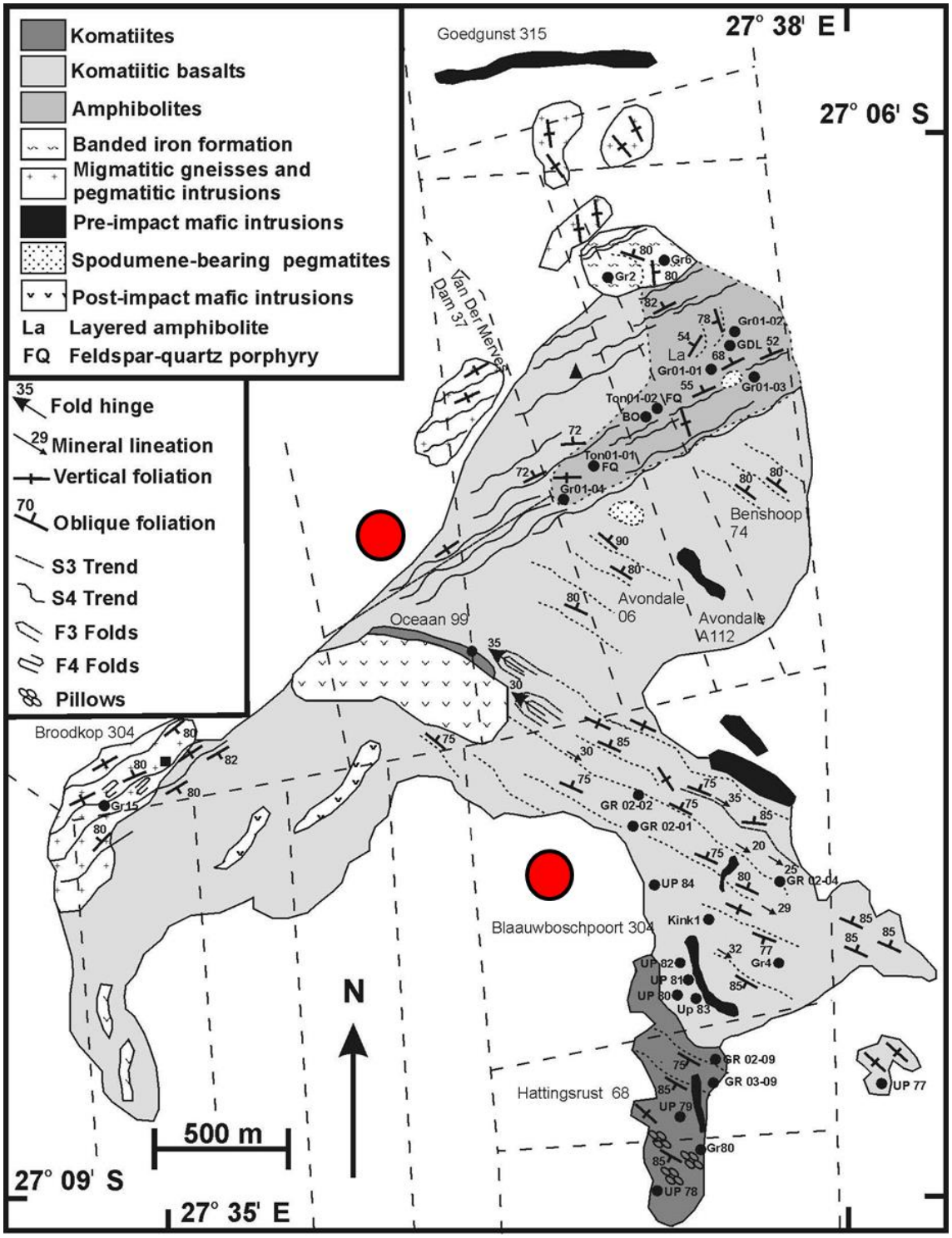


Figure 5:Geological map of the Greenlands Formation. The dotted lines represent the farm boundaries, while the wavy lineaments represent the trend of the Broodkop shear zone. The red circles illustrate the bentonite deposits located on the farm Blaauwboschpoort and Oceaan (From: Lana *et al*., 2003).

2.6. Closing comment

Bentonite deposits are generally related and traced to a nearby volcanic event; however as evidenced by intercalated sandstone and bentonite beds of marine origin in the USA, or the fluvio-lacustrine successions in Tanzania (Dill, 2010), the link between volcanism and the occurrence of bentonite deposits is not always identifiable (Dill, 2010). The Koppies bentonite deposits are spatially distant from any recorded volcanic event. This gives rise to a gap in the literature as to whether these deposits are related to the Greenlands Formation or a distant volcanic eruption. The following chapter describes the methodology and various analytical techniques employed.

Chapter 3

Methodology and analytical techniques

3.1. Introduction

The objective of this chapter is to outline the methodology used in this study and detail the various scientific methods and analytical techniques employed. The methodology of investigation is divided into four stages, namely:

1. *Research* - the review of all available scientific literature with a primary focus on the necessary mechanics, requirements and characteristics of bentonite deposits and their formation. Applicable geology within the study area and a compilation of published literature on the Koppies bentonite deposits was also compiled (as in Chapter 2);
2. *Sample recovery* - sampling of bentonite from the Blaauwboschpoort and Oceaan bentonite deposits including associated overlying sedimentary units;
3. *Physical investigation* - field mapping investigating geological relationships on surface, within open pits and drillholes, focusing on characteristic/anomalous features, outcrops and geological structures;
4. *Sample preparation and analysis* - sample preparation and analysis of results including whole rock XRF analysis, ICP-MS analysis of selected trace element chemistry, scanning electron microscopy (SEM) and cathodoluminescence imaging (CL) of separated zircon grains.

3.2. Sample recovery

Rehabilitation of the Oceaan pit in 2008 did not allow for representative sampling for this study. However, an older individual dataset was obtained, while multiple samples were collected and analysed from the active Blaauwboschpoort pit (Figure 6). A total of nineteen samples were collected between the years of 2006 and 2018 (Table 3). Fourteen of the samples are bentonite, while the remaining samples comprise a quartz precipitate, overlying shale units, topsoil and a mixed shale and bentonite unit overlying the main bentonite seam. The range in depth of samples taken is between 5.4 – 22.8 m.

Samples were obtained 30 - 40 cm beneath the exposed surface to minimise any effects of weathering and contamination. The fresher, relatively unweathered samples were immediately placed into an air-tight sealed sample bag and stored in a temperature-controlled environment until subsequent sample preparation.

Table 3: Synopsis of samples obtained, including associated analytical methods employed.

Year sampled	Sample number	Sample description	Farm name	Co-ordinates (WGS 1984)		Depth from surface (m)	Analytical method				
				Latitude (Y)	Longitude (X)		Major chemistry	Trace chemistry	Mineralogy	SEM	CL
2018	1	Orange waxy Bentonite	Blaauwboschpoort 13	-27.123°	27.616°	12.5	X	X	X	X	
	2	Olive waxy Bentonite	Blaauwboschpoort 13	-27.122°	27.617°	11.2	X	X	X	X	
	3	Grey waxy Bentonite	Ongegund 7	-27.137°	27.608°	21.3	X	X	X	X	
	4	Olive waxy Bentonite	Ongegund 7	-27.138°	27.608°	20.6	X	X	X	X	
2017	5	Olive waxy Bentonite	Ongegund 7	-27.135°	27.608°	5.4					
	6	Orange waxy Bentonite	Blaauwboschpoort 13	-27.123°	27.618°	8.2	X		X		X
	7	Quartz precipitate	Blaauwboschpoort 13	-27.123°	27.619°	6.3	X		X	X	X
2015	8	Bentonite	Blaauwboschpoort 13	-27.124°	27.617°	15.5	X		X		
	9	Bentonite	Blaauwboschpoort 13	-27.124°	27.619°	8.1	X		X		
	10	Bentonite	Blaauwboschpoort 13	-27.123°	27.619°	9.2	X		X		
	11	Bentonite	Blaauwboschpoort 13	-27.139°	27.609°	18.1	X		X		
	12	Bentonite	Blaauwboschpoort 13	-27.141°	27.608°	7.5	X		X		
2013	13	Bentonite	Blaauwboschpoort 13	-27.125°	27.614°	13.2	X		X		
2012	14	Bentonite	Blaauwboschpoort 13	-27.127°	27.617°	16.7	X				
2010	15	Overlying shales	Blaauwboschpoort 13	-27.127°	27.614°	5.2					
	16	Overlying shales	Blaauwboschpoort 13	-27.127°	27.613°	4.6	X				
	17	Top soil	Blaauwboschpoort 13	-27.128°	27.614°	0.2	X		X		
	18	Mixed shale	Blaauwboschpoort 13	-27.128°	27.614°	4.3			X		
2006	19	Bentonite	Broodkop 304	-27.111°	27.597°	22.8	X				

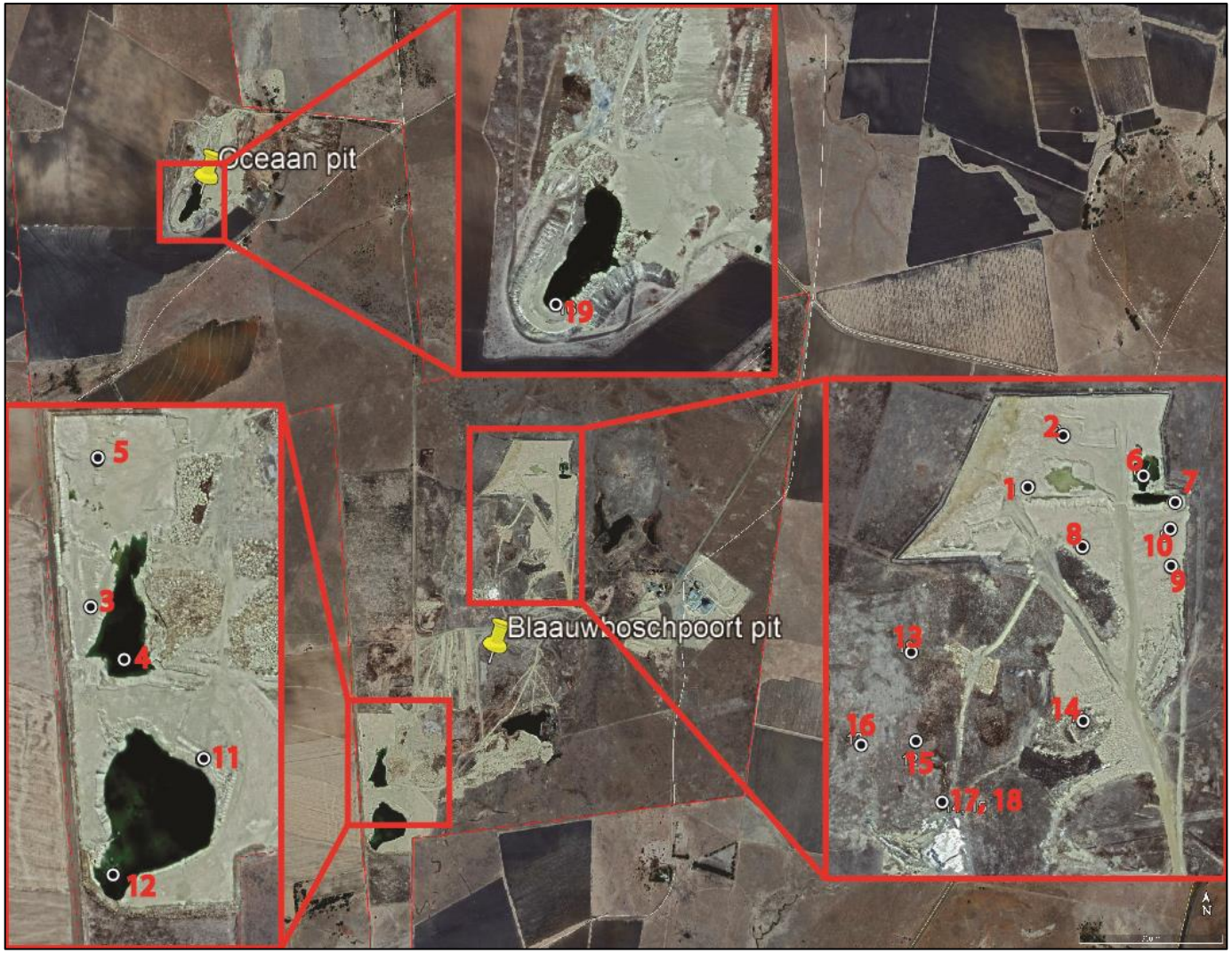


Figure 6: Sample locality map for the samples 1-19 taken from the Blaauwboschpoort and Oceaan deposits and surrounding sub-pits (Google Earth base map image).

3.3. Physical investigation

This phase involved collection of field evidence. Various geological maps sourced from the Council for Geoscience (1:50 000), published journals (Lana *et al.*, 2003, Minnitt and Reimold., 2000) and internal G & W Base and Industrial Mineral Resource field maps (compiled by R. Barnett, P. Ringdal, K. Holliman) were collated and a composite geological map of the area compiled. Further field mapping was undertaken to determine the extent and orientation of the bentonite orebodies and Greenlands Formation. Additional meso-scale structures, associations and contacts associated with the bentonite were also noted.

3.4 Sample preparation and analysis

Sample preparation and analysis was outsourced to Industrial Minerals Consult SA (CC). The methodology and procedures listed below have been provided by J. Horn and is in accordance with accepted industry standards.

All samples initially underwent drying at 40º C in an electric oven for 24 hours with the aim of maintaining an undamaged crystal lattice. The material was then crushed in a jaw crusher to <10mm. Subsequent milling of samples to <75 microns occurred with caution not to overheat or pelletise the clay samples.

3.4.1. X-ray Diffraction (XRD)

Mineralogy of the prepared samples was obtained by means of XRD. Samples were prepared according to the *pressed powder* method*.* Binders were not required due to the inherent properties of bentonite. The samples were analysed with a Bruker D8 Advance X-ray diffraction instrument with Cu radiation.

3.4.2. X-ray Fluorescence (XRF)

Chemistry of samples was obtained via XRF. Representative samples were dried for 3 hours at 100º C and roasted at 1000º C for 3 hours to oxidise Fe^{2+} and S which are detrimental to the Pt used to prepare the glass disks. The loss on ignition (L.O.I.) and moisture was determined gravimetrically during the drying and roasting steps. Glass disks are prepared by fusing 1 g roasted sample and 10 g flux consisting of 49.5 % $Li_2B_4O_7$ 49.5% $LiBO_2$ and 1% Li Br at 950º C. The disks were analysed for major elements by a PANalytical Axios X-ray Fluorescence spectrometer equipped with a 4 kW Rh tube. Trace element analyses required 12 g of milled sample, mixed with 3 g of Licowax, and pressed into a powder briquette by a hydraulic press. The pellets were analysed by a PANalytical Zetium X-ray Fluorescence spectrometer equipped with a 4kW Rh tube.

.

3.4.3. Scanning Electron Microscopy (SEM)

Petrography of the samples was obtained by SEM. Preparation of material involved representative samples being stored in a desiccator for two days to limit any possible charging during the study by maintaining a low moisture state. Samples were analysed using north-south traverses at magnifications varying from 250x to 14 000x.

3.4.4. Heavy Mineral Separation and Cathodoluminescence (CL)

Heavy mineral separation required bulk samples to be crushed and milled in a tungsten carbide disc mill, followed by 250 µm and 500 µm mesh screening. Samples were then washed, decanted and dried followed by traverses with a magnet - a Frantz magnetic separator was used to remove magnetically susceptible zircons which could yield discordant results for subsequent dating (Sircombe and Stern, 2002). Random hand-picking of remaining grains was employed with no preference on size, morphology, or inclusion density to obtain representative samples of the entire zircon population (McKay *et al*., 2016). The selected grains were mounted in a 25 mm block of epoxy resin and polished. A SEM (different from SEM in 3.4.3.) with a cathodoluminescence imager attached was used to record microstructures, cracks, inclusions and other complexities within the zircon grains (Tucker *et al.*, 2013, Corfu *et al.*, 2003).

3.5. The authors contribution

The author was responsible for the verification of field evidence compiled in the composite map, and the collection of samples from 2015 onward. The direction and decision of various analytical techniques employed was the sole decision of the author. While not directly responsible for the laboratory work, the author performed quality checks on the external methods and results by running duplicate samples.

Chapter 4

Results

4.1. Physical investigation and field observations

The Oceaan and Blaauwboschpoort deposits, illustrated as turquoise polygons in Figure 7, are separated by a watershed and appear to have developed within palaeo-lows and meso-scale embayments around the Greenlands Formation within the micaceous shales of the Volksrust Formation. Other minor bentonite occurrences have been marked on Figure 7 and conform to similar trends. The area is largely devoid of exposures of outcrop lending to the extrapolation of contacts between available outcrops. On surface there are no indicators for the presence of bentonite as the anastomosing seams terminate 2 - 4 m from surface. The orebodies represent flat lying to lenticular deposits which are elongated and strike in a northwest-southeast direction.

The uppermost unit within the stratigraphy (Figure 8a) of the Blaauwboschpoort bentonite deposit is a surficial black turf horizon which ranges from 0.5 - 1.5 m below surface. The turf contains variable clay, as evidenced by a slow infiltration rate during the rainy season. Micaceous shales dominate the stratigraphy from 1.5 - 14 m in depth while some intermittent carbonaceous shales (also Volksrust shales) have been recorded interlayered with the former. These atypical Volksrust shales comprise the hanging wall of the deposit. Within the micaceous shale layer, thin bentonite seams or “stringers” of 20 – 50 cm typically occur 10 - 12 m from surface. These “stringers” are observed as good indicators of a deeper, thicker main seam of bentonite. The anastomosing bentonite main seam can occur as significantly thick seams usually ranging from < 0.5 – 2.0 m in thickness or as multiple seams within thinner stratigraphic intervals. On average, the bentonite seams occur at approximately 14 m below surface (mbs), however depths of up to 30 m have been recorded. The footwall comprises a sharp basal contact which ranges from micaceous, sandy or carbonaceous shale. A noticeable absence of sulphide bearing horizons is noted.

The Oceaan and Blaauwboschpoort deposits are similar in depth, thickness, quality and associated sedimentary (host) rocks. Both deposits are devoid of any silicification above or below the main seam of bentonite or “stringers”.

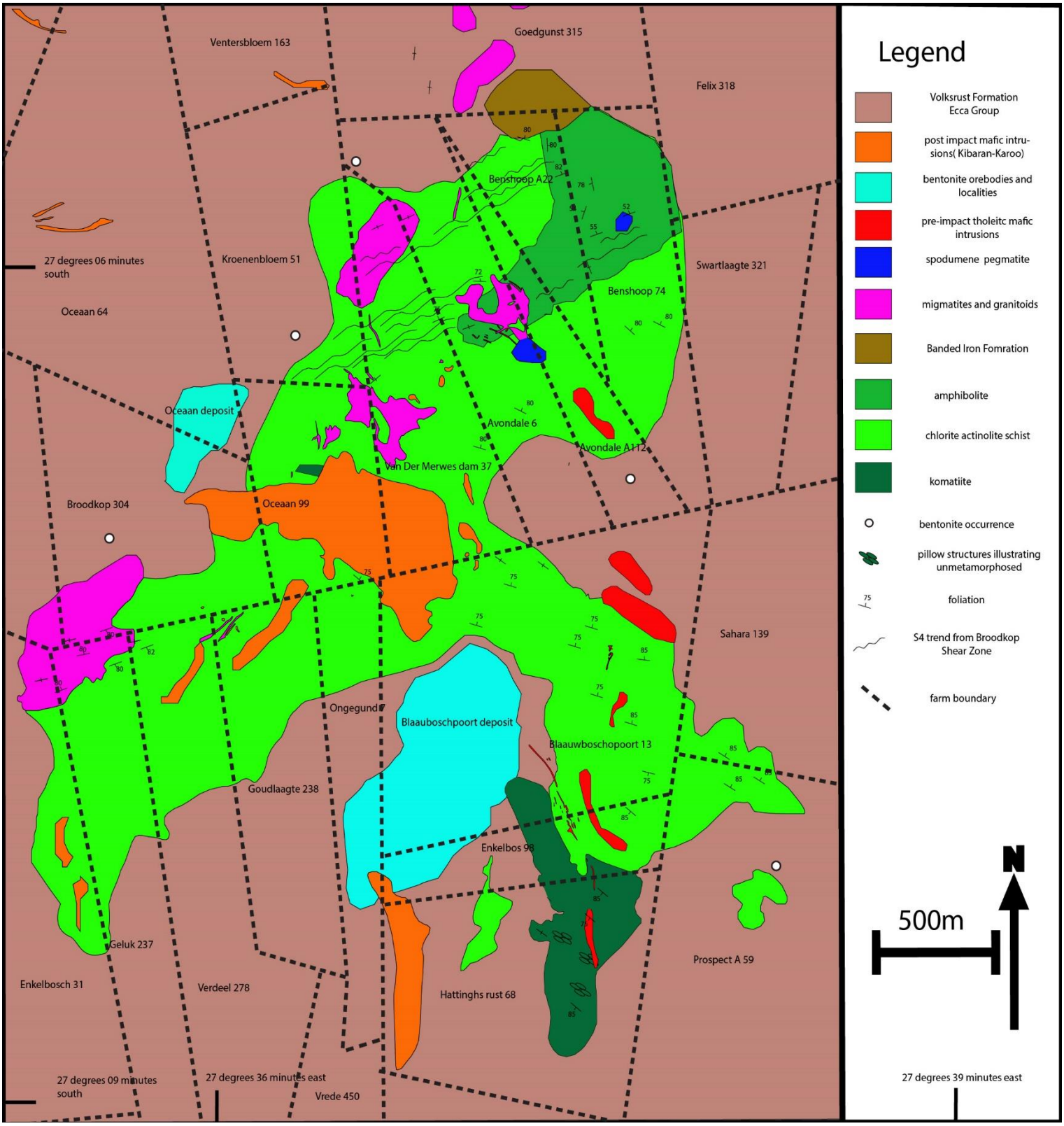


Figure 7: Composite geological map of the Greenlands Formation with the location of various bentonite deposits and occurrences.

In hand sample and *in-situ*, the bentonite has a waxy texture, while weathered exposures exhibit a characteristic 'popcorn' texture. A yellowish-orange bentonite and light-grey to light-khaki brown variety (Figure 8b/8c) both exist, however are restricted to the shallower and deeper sections of the deposit respectively. The variance in colour is a result of oxidation of Fe by surficial and meteoric waters percolating into the shallow portions of the orebodies.

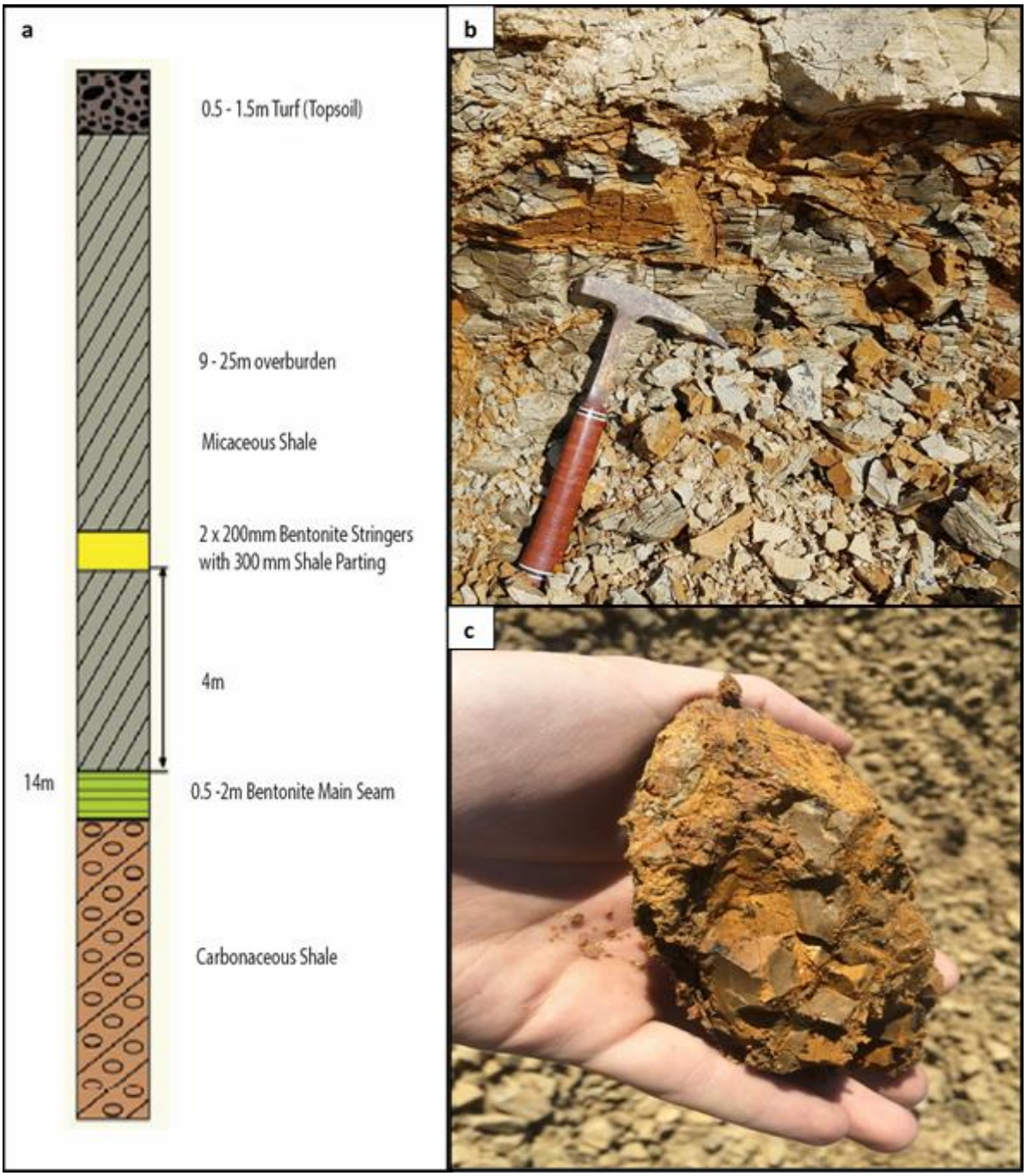


Figure 8: Stratigraphy and field evidence of the Koppies bentonite deposits. (a) Stratigraphic column, (b)*In-situ* khaki brown to grey bentonite seam identified as sample 2, the darker colour is due to characteristic water retention in comparison to overlying micaceous shales, (c) Structureless, and waxy orange bentonite near Sample 6 illustrating the colloidal nature. Notable manganese growths are evident.

Calcium carbonate and silica veins, nodules and boxwork concretions (Figure 9a) are present throughout the Koppies deposits and are restricted to a maximum depth of 7 meters below surface (mbs). Dendritic manganese oxide growths (Figure 9b) occur on the surface of the bentonite along planes which exhibit increased water flow. Remaining inclusions within the Koppies bentonite are limited to acicular growths of authigenic, manganiferous barium sulphate and siderite. The inclusions can range in size from small 5 cm acicular growths to large 2 m wide dense concretions. The larger concretions contain a barium-rich core with outward sideritic growth (Figure 9c and d). There is a relationship with regards to increasing diameter of concretions and depth of bentonite in which they occur.

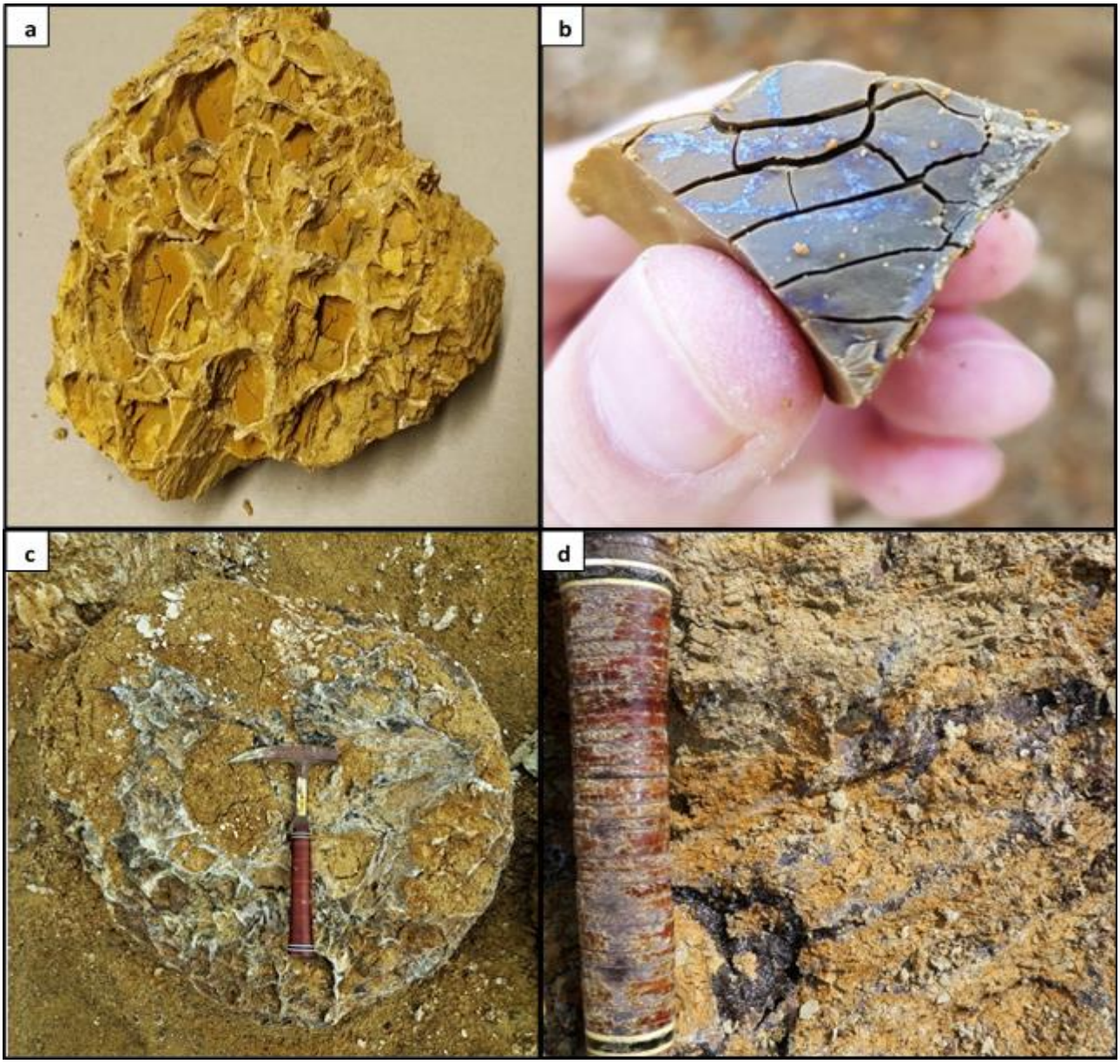


Figure 9: Field evidence and various inclusions within the Koppies bentonite deposit. a) Sample 7 showing boxwork quartz precipitate found within shallow extent of bentonite orebody. b) Dendritic manganese oxide growth in cracks within khaki brown bentonite at Sample 5 locality. c) Irregularly shaped, large barium-rich siderite concretion formed within the bentonite at Sample 4 locality. d) Bentonite present on outer surface of siderite concretion.

Post-bentonite igneous intrusions have been recorded at the Blaauwboschpoort deposit which have effectively sterilised the bentonite from a mining perspective. The sporadic contact between the bentonite and limited intrusions of doleritic sills and dykes are characterised by a friable weathered zone. Associated hydrothermal fluids are believed to have altered nearby *in-situ* bentonite and shales in portions of the deposit. The increased temperatures associated with the intrusions result in an irreparably damaged crystal lattice. This alteration is evidenced as a hard, devitrified olive-green, “burnt” bentonite and a dark blue, indurated shale devoid of any original physiognomies. Whilst most bentonite deposits illustrate a weathering profile from volcanic glass to smectite, the Koppies deposit contradicts this trend, as allophane or intermediate minerals are completely absent throughout the deposits.

4.2. Petrographic observations

4.2.1 SEM

Samples 1 - 4 of bentonite under the scanning electron microscope comprise aggregated, poorly-crystalline, small, wavy flakes of montmorillonite which appear as a thin crust. The various forms of smectite present are curly to crenulated flakes on the crust (Figure10a) and booklet-type stacks (Figure 10b) of montmorillonite grains. The curly, crenulated montmorillonite flakes are indicative of collapsed morphologies, which are most likely due to the drying and desiccation process during sample preparation, while the euhedral flakes form foliated lamellar aggregates with face to face associations. Various recently smoothed faces of montmorillonite grains are also evidenced within the matrix and are indicative of second-generation flakes which are located in shrinkage cracks and cavities.

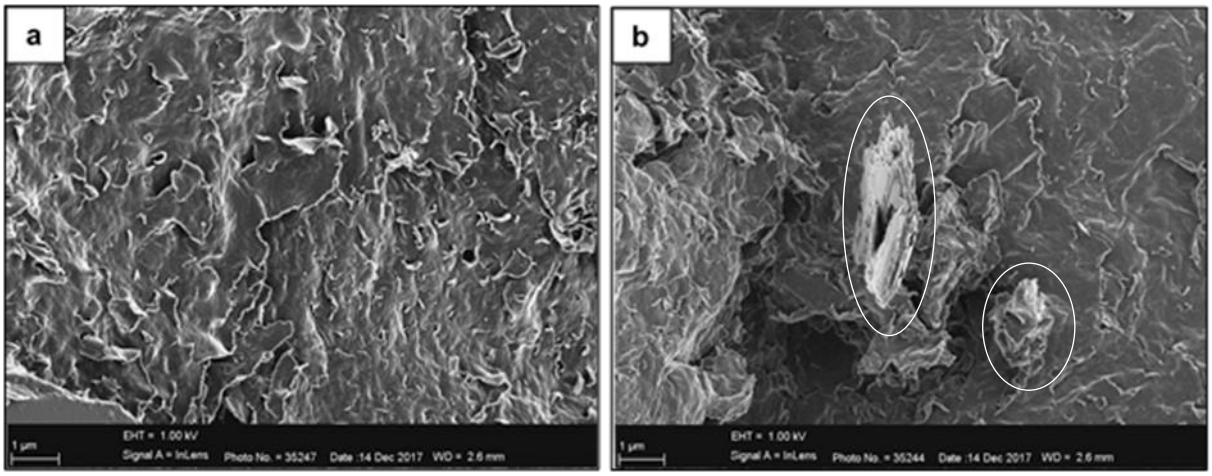


Figure 10: Scanning electron photomicrographs of smectite textures observed in the Blaauwboschpoort bentonite. (a) Smectite dominated matrix illustrating crenulated edges of the flakes. (b) Booklet, face to face associations of smectite flakes (circled in white).

Voids within the smectite matrix are observed in Figure 11a and may suggest the loss of rounded comparatively hard grains during the sample preparation stage. One sub-euhedral to euhedral zeolite grain was noted within the montmorillonite matrix (Figure 11b).

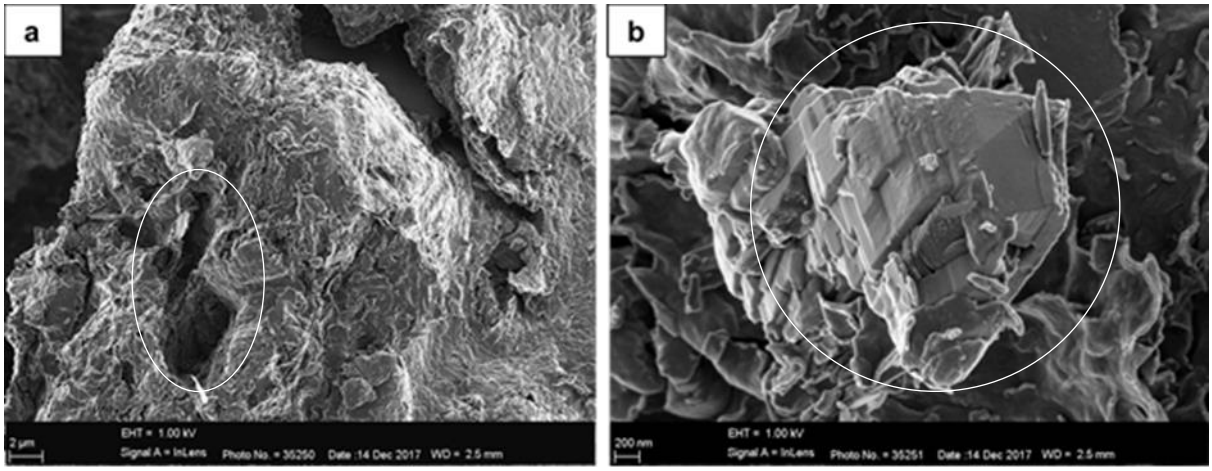


Figure 11: Scanning electron photomicrographs of inclusion minerals within the smectite matrix observed in the Blaauwboschpoort bentonite. (a) Void in the smectite matrix illustrating a remnant rounded quartz crystal (circled in white), (b) Individual zeolite grain amongst smectite mass (circled in white)

In sample 7, a quartz boxwork precipitate within the shallow extent of the Blaauwboschpoort bentonite seam was analysed (Figure 12a and b). The quartz grains are sub-euhedral to euhedral crystals with a gel-type precipitate on the crystal surface. A clear contact between the bentonite and quartz exists.

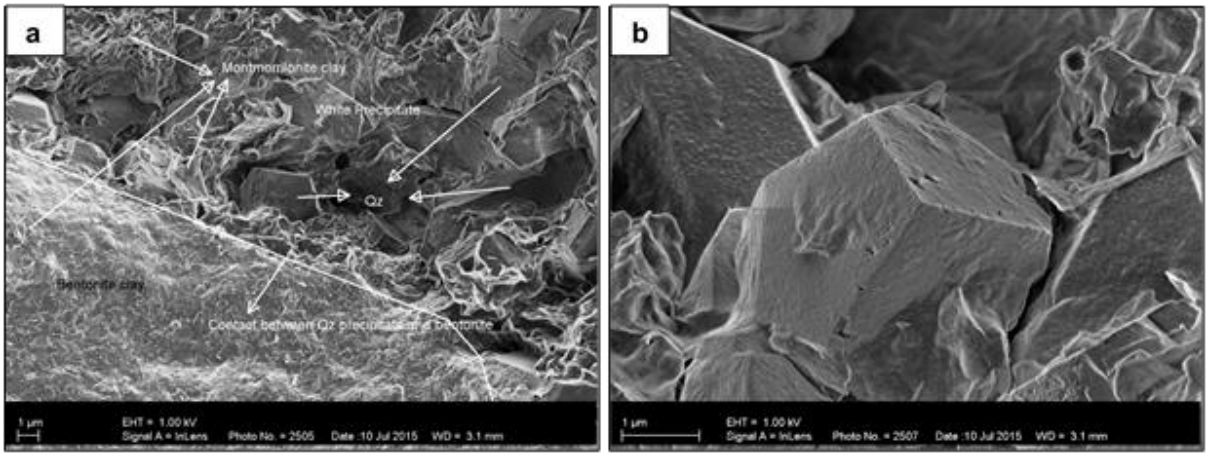


Figure 12: Scanning electron photomicrographs of the boxwork quartz and bentonite contact within a pre-existing crack within the Blaauwboschpoort bentonite deposit (a) Sharp contact between the quartz precipitate and bentonite (annotated in white), (b) Zoomed-in angular quartz crystals with smectite surface coatings.

4.2.2. Heavy mineral recovery and cathodoluminescence

The CL images are a part of another ongoing study and have been included in this study with permission. See acknowledgments at page v for more details.

The heavy minerals obtained from the Blaauwboschpoort bentonite vary in shape and range in size from 20 - 100 µm in length (Figure 13). Abundant small euhedral zircon and apatite grains dominate while a small set (less than 5 %) of large zircon crystals are present. The larger crystals can be described as rounded or fragmentary while smaller crystals occur as elongated needles to short and stubby varieties, with minor rounding. The majority of zircon crystals are colourless and contain fine oscillatory zoning while core and rim textures are less frequent.

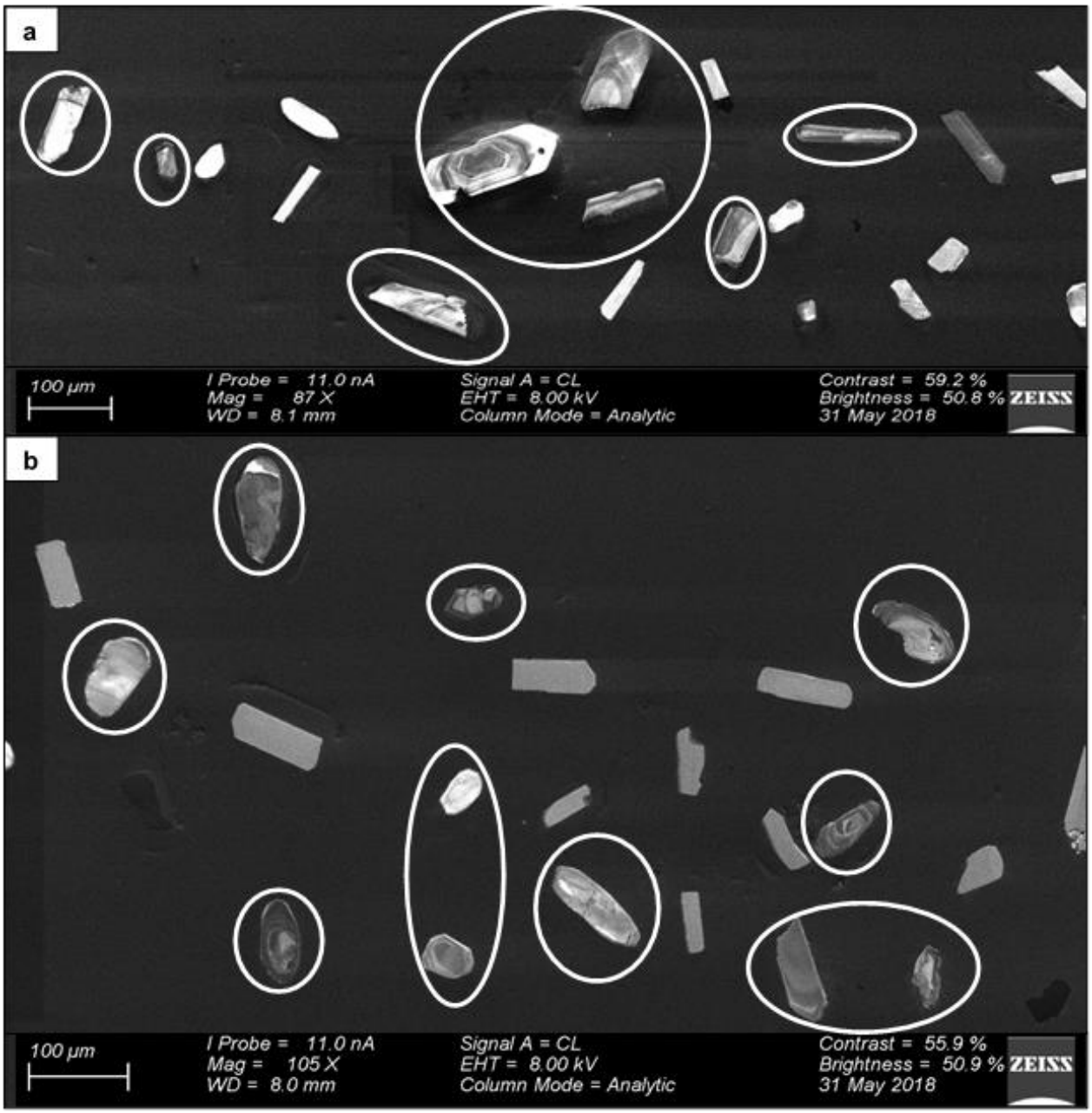


Figure 13: Recovered grains of fragmented, elongated, stumpy, large, small and zoned heavy minerals from the Blaauwboschpoort bentonite. White circles illustrate the zircons while the remainder of crystals represent apatite grains (87x magnification). (a) Zoned euhedral zircon crystals. (b) Fragmented, rounded zircon crystals.

4.3. Data Presentation

4.3.1. Geochemical results for major and trace elements

The geochemical results of the seventeen samples from the Koppies bentonite deposits are represented in Table 4. As per the sampling synopsis table, samples 1 - 6 and 8 - 14 are bentonite sourced from the Blaauwboschpoort deposit, followed by samples 15 – 16 comprising the overlying shales and sample 19 from the Oceaan deposit. Both deposits have MgO and CaO as the dominant cations, while Na_2O is noticeably depleted in relation to other cations. The Mg:Ca ratio for Blaauwboschpoort is 2.26, 3.4 for Oceaan and 1.9 for the overlying shales. The loss on ignition (LOI) ranges between 7.1 - 14.56 % for the bentonite samples and 5.5 - 6.5% for the shale samples.

The Oceaan deposit contains slightly elevated SiO_2 and depleted Fe_2O_3 and TiO_2 when compared to the Blaauwboschpoort deposit, while the overlying Volksrust shales are enriched in SiO_2, K_2O and Na_2O and depleted in Al_2O_3 and MgO in relation to the Koppies bentonites. The southern, deeper samples in the Blaauwboschpoort deposit, namely samples 11 and 12 have slightly enriched SiO_2 figures in comparison to the shallower portion of the deposit.

As per the sampling program only four samples from the Blaauwboschpoort deposit were sampled and analysed for selected trace element chemistry (Table 5) with a focus on Ba, Nb, Nd,Ti, Zr and Y.

4.3.2. Mineralogy of the Blaauwboschpoort and overlying shales

Smectite dominates the mineralogy with a range of 84 – 99 %, while quartz ranges from 1 – 9 %. Accessory minerals include mica, chlorite/kaolinite, plagioclase, calcite and K-feldspar. The surficial turf soil layer is comprised of 80 % quartz with minor smectite, while the overlying mixed shale and bentonite layer contains equal parts smectite and quartz with significant plagioclase.

Table 4: Quantitative major geochemical results of the Blaauwboschpoort and Oceaan bentonite and overlying shale samples.

Major Element (%)													
Sample no.	SiO_2	TiO_2	Al_2O_3	Fe_2O_3	CaO	MnO	MgO	K_2O	Na_2O	P_2O_5	Cr_2O_3	LOI	TOTAL
1	55.78	0.48	18.95	9.22	1.68	0.08	4.33	0.54	0.13	0.04	0.01	9.33	100.57
2	57.54	0.51	19.37	7.17	1.76	0.06	4.18	0.83	0.15	0.04	0.01	9.00	100.62
3	58.42	0.35	19.76	6.98	1.89	0.04	3.77	0.35	0.11	0.01	0.01	9.17	100.84
4	56.89	0.34	20.24	6.99	2.21	0.10	3.77	0.37	0.11	0.04	0.01	9.70	100.77
5	59.06	0.60	19.15	6.99	1.94	0.03	3.20	1.07	0.29	0.05	0.02	7.10	99.50
6	55.79	0.56	19.86	8.03	1.85	0.06	4.40	0.74	0.14	0.16	0.02	7.90	99.51
8	56.56	0.44	20.34	7.35	1.49	0.02	4.25	0.54	<0.01	0.15	0.01	8.60	99.75
9	55.79	0.45	20.39	7.38	1.71	0.17	4.30	0.60	0.02	0.13	0.01	8.84	99.80
10	54.42	0.45	20.26	8.59	1.56	0.04	4.33	0.55	<0.01	0.15	0.01	9.12	99.48
11	57.56	0.54	19.41	5.68	2.63	0.07	3.06	0.92	0.34	0.07	0.01	9.84	100.13
12	56.19	0.38	18.68	6.08	1.52	0.04	3.49	0.54	0.12	0.05	0.01	12.89	99.98
13	53.94	0.34	18.23	6.75	1.26	0.08	4.04	0.46	0.11	0.08	<0.001	14.56	99.86
14	59.14	0.34	19.03	6.96	1.88	0.05	3.75	0.36	0.07	0.07	0.01	8.87	100.52
15	65.31	0.66	15.80	3.84	1.20	0.10	2.35	2.73	1.13	0.21	0.04	5.51	98.89
16	63.23	0.71	16.78	5.32	1.35	0.06	2.50	2.63	0.88	0.15	0.04	6.50	100.15
19	61.58	0.23	18.89	3.58	1.32	-	4.54	0.43	0.25	-	-	8.80	99.62

Table 5: Quantitative selected trace geochemical results of bentonite from the Blaauwboschpoort deposit.

Trace Elements (ppm)				
Sample no.	**1**	**2**	**3**	**4**
As	12	3	2	7
B	25	29	28	40
Ba	226	164	279	407
Be	5	5	4	4
Ce	55	63	44	50
Co	28	21	10	17
Cr	67	61	59	21
Cs	8	16	1	1
Cu	50	19	173	47
Ga	69	68	61	62
Ge	1	1	1	1
Hf	12	12	14	14
Ho	1	1	1	1
La	106	112	59	85
Li	35	40	27	24
Mn	2264	1584	1112	3743
Mo	1	0	0	2
Nb	24	30	29	28
Nd	71	73	36	54
Ni	36	26	51	19
Pb	145	65	29	152
Rb	3	5	2	1
Sb	2	1	1	1
Sc	12	11	12	11
Sn	8	8	9	9
Sr	259	241	245	209
Ta	4	4	3	3
Th	43	46	39	52
U	3	3	4	7
V	194	136	95	64
W	5	6	4	2
Y	40	40	20	40
Zn	278	220	160	226
Zr	369	342	433	445

Table 6: Semi-quantitative mineralogical data of the Blaauwboschpoort bentonite, overlying shale and topsoil.

Sample no.	Smectite	Qtz	Mica	Chl/Kaol	Plag	Cal	K-feldspar	Illite-Montmorillonite
1	97	3	-	-	-	-	-	-
2	96	4	-	-	-	-	-	-
3	96	4	-	-	-	-	-	-
4	95	3	-	-	-	2	-	-
5	87	9	-	3	-	-	-	-
6	99	1	-	-	-	-	-	-
8	98	1	1	-	-	-	-	-
9	**98**	**1**	**1**	**-**	**-**	**-**	**-**	**-**
10	97	1	2	-	-	-	-	-
11	85	8	2	3	1	-	1	-
12	84	9	3	0	4	-	trace	-
13	98	2	-	-	-	-	-	-
17	11	80	-	-	2	1	1	4
18	41	41	4	2	10	-	2	-

4.4. Closing comment

While an individual result may be pertinent in its own right, the combination of evidence sourced from various analytical techniques shape an unbiased interpretation of the processes responsible for the formation of the Koppies bentonite deposits.

Chapter 5

Interpretation

5.1. Relationship between the Koppies bentonite and Greenlands Formation

Based on the absence of a gradational alteration profile or allophane material, the Oceaan and Blaauwboschpoort deposits are unlikely to have formed as a result of the chemical alteration of rocks within the Greenlands Formation. Field evidence confirms that the bentonite does not make contact with the Greenlands Formation rocks. Similarly, the Greenlands Formation does not appear to have been chemically altered or remobilised. This suggests that the bentonite is likely derived from an external source such as an ash fall-out event and not the *in-situ* weathering of the Greenlands outlier. Therefore, an exclusive focus on the classification and interpretation of only the bentonite deposits is explored further.

5.2. Geochemical perspectives

There is sufficient evidence to suggest that the Koppies bentonite samples have undergone a multitude of processes in their formation. The aim of this section is to use the geochemical results to propose the major processes which are responsible for the neoformed bentonite, as it exists today.

Alteration and conversion of volcanic glass or associated volcanics to smectite involves element mobilisation which is controlled by the interacting fluid (Christidis, 1998). Water properties such as Eh, pH, organic matter content and the amount of Mg in suspension play significant roles during the alteration phase. The favoured mobile elements include low valence, large ions e.g. alkalis, Mg and Si within an alkaline basin. In contrast, immobile elements defined as less soluble, small, high valence ions e.g. Al, Nb, Th, Ti, Y and Zr can only be altered residually (Caballero *et al*., 1992). In this regard, immobile elements can be used to interpret and correlate the source magma while mobile elements can be used as proxies for the effects of secondary processes such as diagenesis or supergene alteration (McKay *et al*., 2016). All geochemical results have been interpreted cautiously as various syn- and post-depositional processes would have acted on both the bentonite and sedimentary rocks. This unavoidably resulted in complex changes to the original geochemical composition (Weltie and van Eynatten, 2004).

Under the hypothesis that a bivariate plot of immobile elements, which represent the same initial composition, exhibits a linear correlation then mobile-mobile or mobile-immobile plots will not correlate nor pass through the origin of the graph (Christidis, 2008). These non-

correlative trends illustrate either uptake of elements as a negative intercept on the y-axis, or depletion of elements as a positive intercept on the y-axis.

Aluminium and titanium oxide, under normal conditions are usually immobile with a low solubility (Smith, 1967). Apart from strongly acid or alkaline environments, the stable oxides frequently produce a correlative bivariate plot. Figure 14 verifies this hypothesis with a slight deviation from the origin of the graph. This deviation can be explained by variations in initial composition of volcanic material, solubility effects and/or the representivity of a small sample set (Christidis, 1998).

During the alteration of bentonite, silica is usually considered mobile with a decrease in concentration with progressive alteration (dos Muchangos, 2006, Galan, 2006). Figure 14 illustrates that Si has been mobilised as the trend is relatively flat, while the intercept is positive. The degree of alteration can be comparatively measured by the Al_2O_3 vs. SiO_2 ratio. A bentonite with fewer impurities would denote a lower ratio while conversely high ratios produce opal-CT and alkaline-rich zeolites (Grim and Guven, 1978). With a ratio of 2.9, the Koppies bentonite represents a pure high-quality bentonite resembling that of the American Wyoming bentonite deposit (Elzea and Murray, 1990), which is largely devoid of impurities.

The remainder of bivariate graphs illustrate that Ca and Mg were enriched, Na was depleted and Fe immobile. Ca and Mg were most likely enriched through uptake from sea or meteoric waters (Berry, 1999). Depletion of Na and Si is likely to have occurred during devitrification of volcanic glass and mobilisation into the Volksrust shales, as evidenced by relatively higher Na and Si values for the shales. The overlying Volksrust shale has the same trend as the bentonite illustrating post-deposition processes which acted on both units.

5.3. Environment

Th/U ratios are usually employed as a measure of oxic vs. anoxic depositional settings as large ion lithophile elements (LILE) are considered unaffected/resistant to alteration (Dypvik and Harris, 2001). The major host mineral for Th in the Blaauwboschpoort bentonite is zircon, which is highly resistant to both physical and chemical weathering. The bentonite samples contain Th/U ratios ranging from 7.4 - 15.3 demonstrating a strongly oxygen-dominated environment which is to be expected during the time of deposition of the Volksrust Formation (Johnson *et al*., 2006).

The presence and ratio of dominant cations have been employed to infer the probable environment under which the precursor-ash was altered (Arslan *et al*., 2010). Although Mg is usually supplied through seawater and Ca is controlled by the parent material, the presence

of Mg and Ca as the dominant cations (Figure 15) suggest both alternating brackish and fresh water conditions prevailed (Calarge *et al*., 2006).

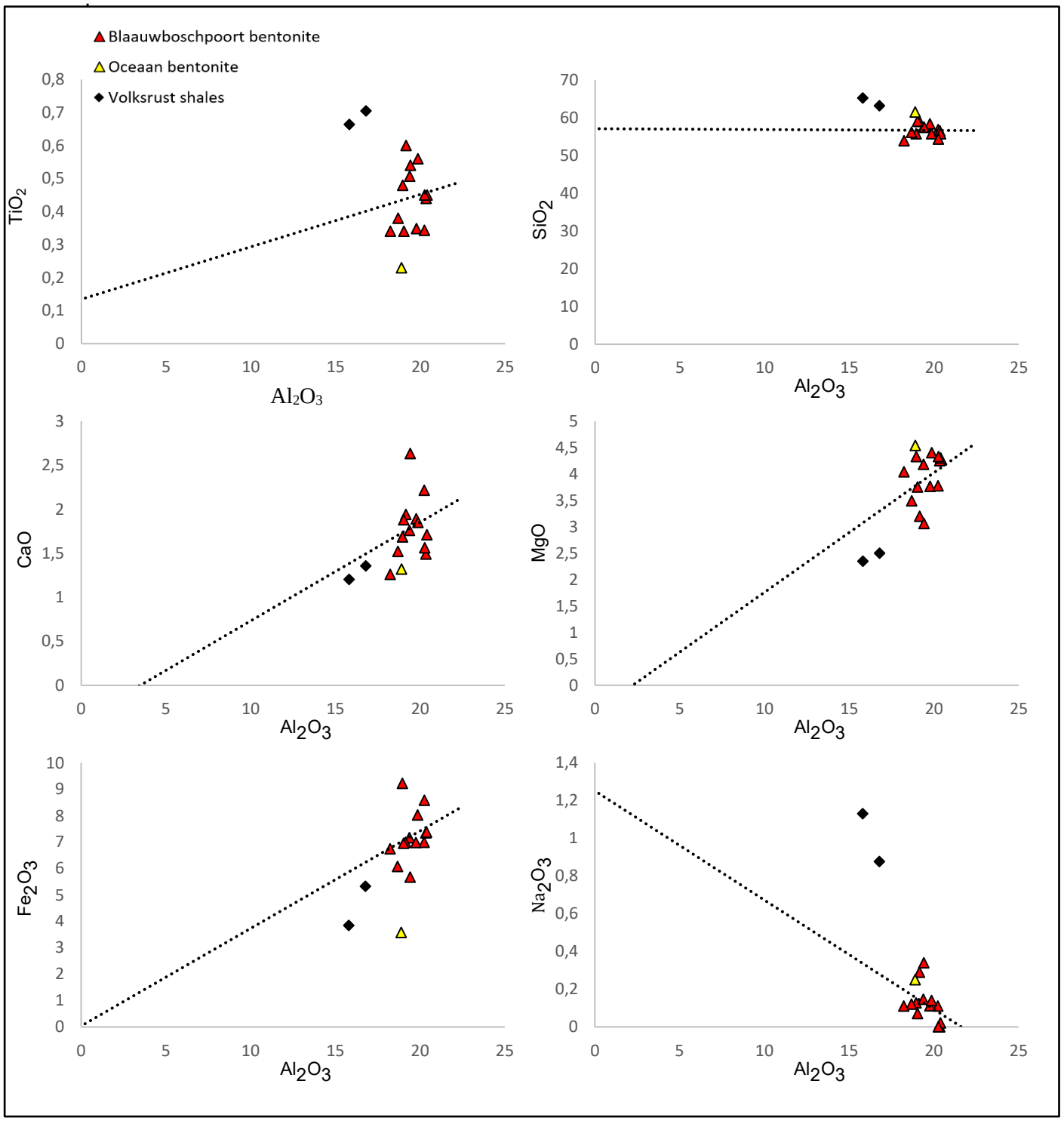


Figure 14: Immobile element Al versus mobile/immobile elements for the Koppies bentonite deposits and overlying Volksrust shales. Trend lines illustrate enrichment as a negative intercept and depletion as a positive intercept for a given element (Christidis, 1998).

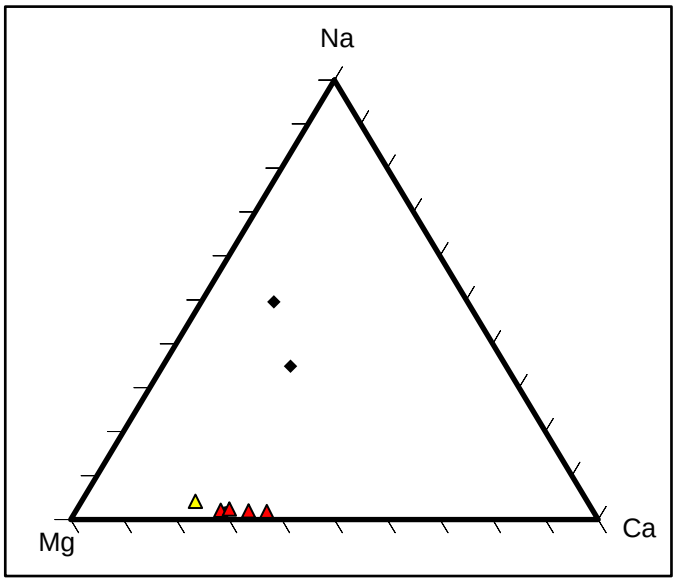


Figure 15: Ternary plot of dominant cations present in the Koppies bentonite in relation to the overlying shales (atypical chemistry of shales). The Koppies bentonite samples reflect a Na depleted array, similar to the Wyoming bentonite deposits (Altaner *et al*., 1984, Knechtel and Patterson, 1962).

5.4. Weathering

The chemical index of alteration graph (CIA), indicating the severity of the weathering process which the precursor rocks underwent, suggests that the Koppies bentonite samples underwent extensive chemical alteration (Figure 16), more severe than the surrounding host Volksrust shales. The Volksrust shale is representative of a weak-intermediate degree of chemical weathering. The strong weathering pattern of the bentonite is characteristic of an interaction with a consistent meteoric water table, oxidation and limited leaching, which promoted chemical alteration (Dill, 2017). The slight differences between the Blaauwboschpoort and Oceaan deposits can be explained by differences within the discrete micro-environments in which they formed as shown in other deposits by Takgati *et al*. (2016). Barium (usually enriched in shales and clays) is relatively stable during initial stages of alteration but becomes more concentrated with increasing degrees of alteration (Caballero *et al*., 2017). The enriched figures of 164 – 407 ppm Ba for the Koppies samples illustrate the maturity of dominant chemical weathering conditions.

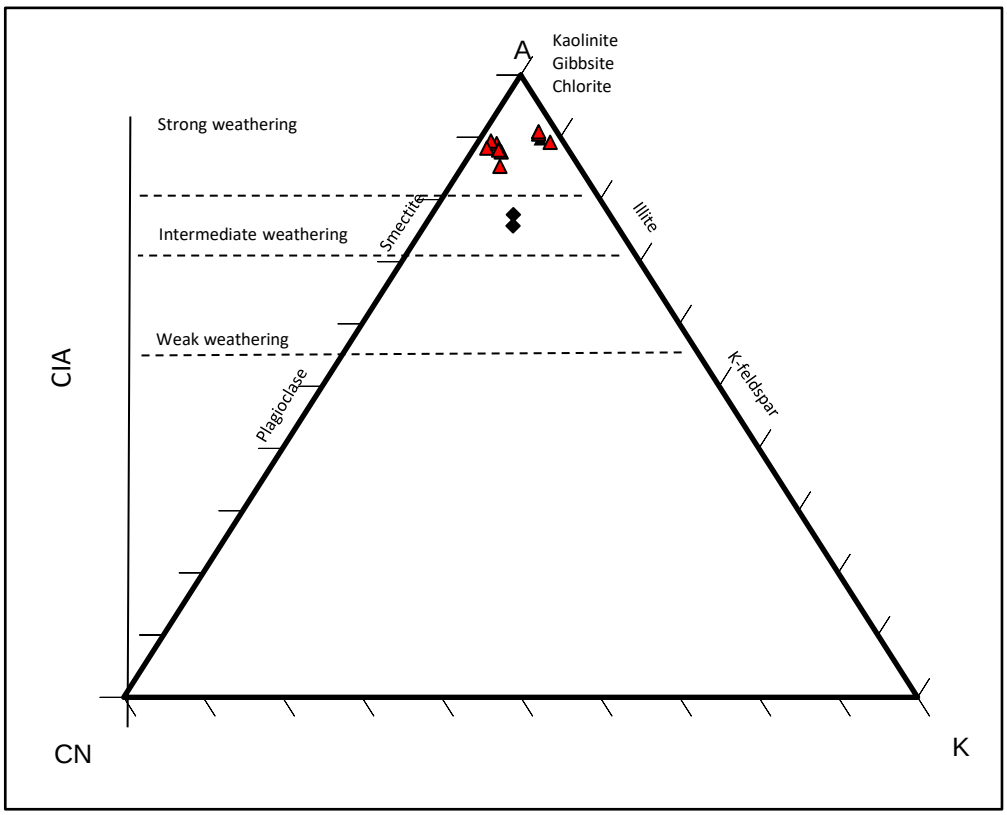


Figure 16: Ternary diagram of A-CN-K, where A = Al_2O_3, C = CaO N =Na_2O, K =K_2O (Nesbitt and Young, 1984). Bentonite plots in strong weathering field while overlying shales plot between the intermediate and weak weathering fields.

5.5. Provenance

When discerning precursor or provenance studies, it is imperative to make use of the immobile elements or at least be aware of elements which signify minor mobility. Discrimination diagrams of Winchester and Floyd (1977) are centred on the immobility of Nb, Ti, Y and Zr within bentonite. Severe alteration can, in some instances, mobilise Y (Christidis *et al.,* 1995). Ratios of Zr/TiO_2 and Nb/Y are also dependent on the abundance of heavy minerals, such as zircon, anatase, rutile, ilmenite, and monazite. These minerals are a result of either fractionation during aeolian transport or water settling, or due to mixing with enclosing detrital shales containing zircon and other heavy minerals inherited from a protolith (Pellenard *et al*., 2003).

The Blaauwboschpoort bentonite samples, shown in Figure 17a, are averaged as a trachyandesite composition comprising a range of felsic to intermediate rocks such as rhyolite, trachyandesite, rhyodacite/dacite and trachyte. The horizontal scatter is most likely a result of variable detrital input of clastics and/or the effects of leaching.

The tectonic setting discrimination diagrams (Figure 17b) reflects a scattered pattern, plotting predominantly in the ‘intra-plate’ granite field with one sample plotting in the volcanic-arc

granite field. In combination, the high Zr, low Co, Th/Sc, Ti/Zr and La/Sc ratios suggests that the precursor material was derived from a passive extensional margin (Bhatia and Crooke, 1986).

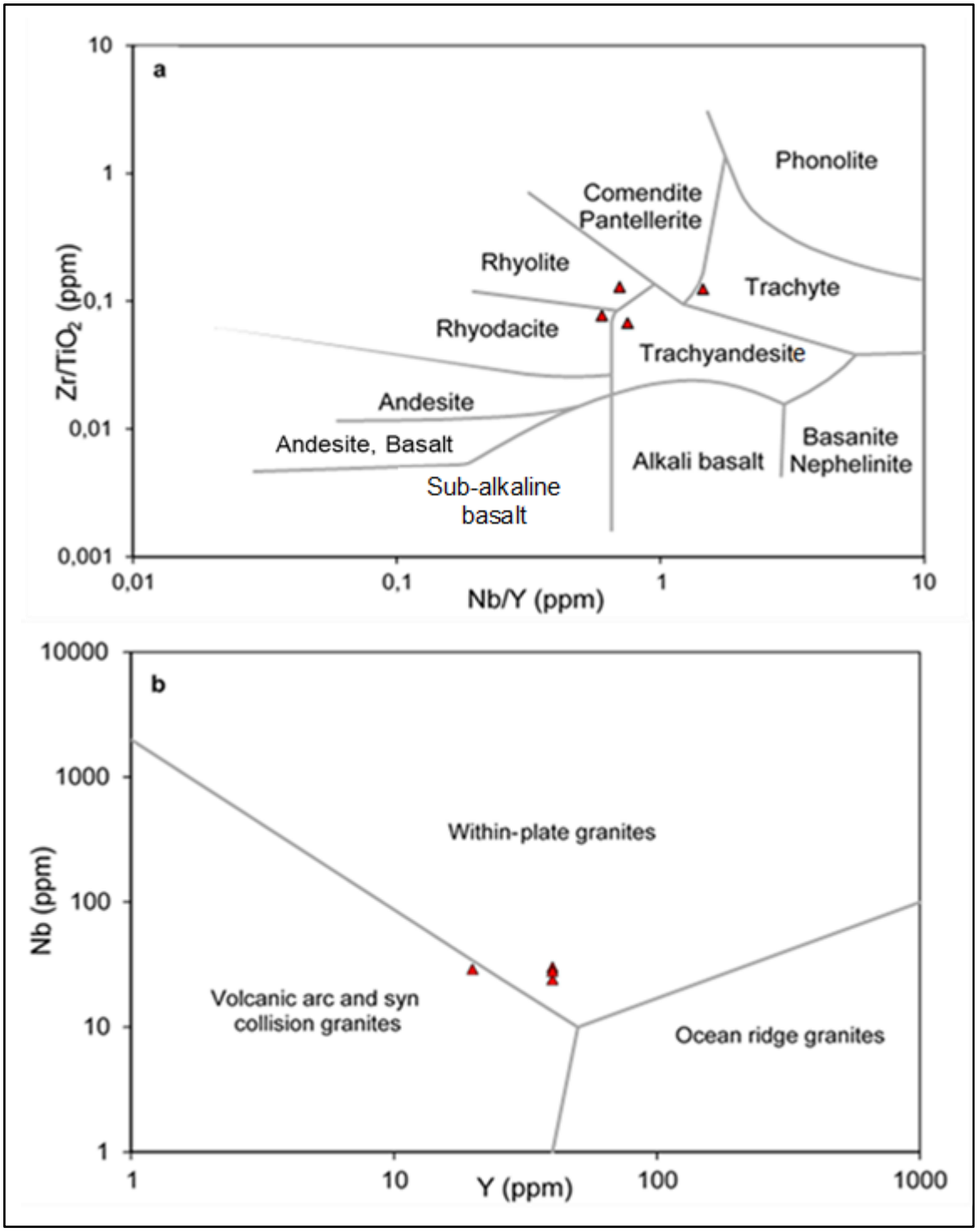


Figure 17: Bivariate trace element plots for the Blaauwboschpoort bentonite deposit. (a) Rhyolitic character versus alkalinity graph (Winchester and Floyd, 1977). (b) Discrimination diagram of Nb vs. Y (Pearce *et al.*, 1984)

5.6. Optical interpretations

The absence of pseudomorphic textures, usually represented by angular, sharp-edge fragments, and lack of remnant volcanic textures or early-phase alteration minerals, such as amorphous glass or cristobalite within the samples is suggestive of a non-volcanic source (Henderson, *et al*., 1971). It is important to note that the degree/severity of alteration experienced by the bentonite is also considered to be a prominent overprinting mechanism, obscuring the primary mechanism of formation (Christids, 2008). The presence of an individual zeolite grain can be inferred to be a low temperature clinoptolite rather than a medium temperature mordenite or high temperature analcime based on the low temperature range 100 - 300ºC, in which the bentonite was most likely formed (Christidis, 2001).

Bentonite deposits derived from volcanic ash usually contain a large variety of zircon morphologies which can range externally in size and shape and internal structures (Corfu *et* al., 2003). Under idealised conditions, rapid and synchronous crystallisation of zircons in the magma chamber prior to, or during, a volcanic eruption yield small, euhedral grains. This is considered the simplest to interpret as all zircons would theoretically contain identical shapes and colours. The majority of zircons from the Blaauwboschpoort pit are small and colourless with little variation suggesting a possible single source; however, a moderate variation in shape is observed. The orientation of oscillatory zoning, with no core and rim textures, illustrate multiple periods of zircon growth, while other grains suggest a single magmatic crystallisation episode based on the lack of zoning (McKay *et al*., 2016). Volcanic ash deposits are rarely devoid of foreign zircons as active fluvial/lacustrine currents add an element of lateral transport to external inherited zircons, usually manifesting as anomalous inherited large, rounded and rare zircon grains (Corfu *et al*., 2003). The above-mentioned characteristics, combined with a mineralogy dominated by smectite, suggest a single-source ash event deposited in a basin, with the influx of surrounding detritus, subsequently altered under a low-temperature environment.

Chapter 6

Discussion: Formation of the Koppies bentonite deposits

The aim of this chapter is to propose a site-specific, deposit-scale description for the formation of the Koppies bentonite deposits. This discussion details the source, transport/deposition and alteration of the Koppies bentonite deposits based on the findings of the previous chapters.

6.1. Permian ash deposits

The Permian signified a period of numerous worldwide, explosive Plinian eruptive events resulting in the transport and deposition of fine ash layers over thousands of kilometres, most notably within the northwest portion of the MKB (Huff, 2008). Geochemical data on Permian tuffaceous beds, volcanics (ignimbrite and lava bombs - base of Beaufort Group) and bentonites have been compared (Bordy and Abrahams, 2016; Viljoen, 1994; McLachlan and Jonker, 1990; Keyser and Zawanda, 1988; Lana *et al.*, 2003). The evolution of models attempting to resolve the source of the ash occurrences are detailed below:

- ash fall-out deposits (ignimbrite and lava bomb samples) near Frankfort in the Free State Province of South Africa are noted as acidic volcanic pyroclastics (ignimbrites) were believed to have been transported from the north, based on evidence of south-directed palaeo-currents in the host sedimentary rocks, however the volcanic source has not been identified (Keyser and Zawanda, 1988);
- analyses on glass-shard sizes of several ash and bentonite occurrences in the northwest Karoo suggested a proximal source for the ash based on the calculated distance travelled (McLachlan and Jonker, 1990); and
- tuffaceous and bentonitic beds were deposited during the transgression of the Volksrust Formation and believed to have been transported from the (south) southwest, based on sedimentary structures in the host rocks (Viljoen, 1994).

6.2. Source

The Koppies bentonite can be linked to an anorogenic ‘within-plate granite setting’, where voluminous, tuffaceous trachyandesitic ash plumes were produced. The scatter in the observed chemistry is likely to be as a result of an increase in sedimentation rate or input of externally-sourced detritus during deposition (Puspoki *et al*., 2005). However, in areas with abundant water/rock interactions, it has been postulated that this may serve to homogenise differences in the composition of parent rocks (Christidis, 2001). Trachyandesite is similarly

considered the favourable precursor for the formation of high-quality di-octahedral bentonites as acidic precursor rocks, while high SiO_2:Al_2O_3, tend to produce zeolites instead (Chrisitidis, 2008). The preponderance of small, colourless zircon populations further suggests a single ash source, with the presence of rare, large, rounded grains attributable to the input of externally sourced detritus during the depositional phase, recycled or inherited zircon grains (McKay *et al*., 2016). The lack of opal-CT and zeolites within the neoformed bentonite suggest that the ash fallout originated from a distant volcanic event, not limited to sub-Saharan Africa, based on the minimal thermal contrasts evidenced during initial interaction between the ash and interacting water (Christidis, 2008).

While Early to Middle Permian (>270 - 260 Ma) tuffaceous units of the Karoo are linked to a subduction magmatic arc setting, Late-Permian (<265 Ma) tuffs are associated with intraplate shallow source magmatism in an extensional setting (McKay *et al*., 2016). As the source of ash for the Koppies deposit is constrained to the Late Permian, a possible tectonic source within Gondwanan history may be identified (McKay *et al*., 2016)

The Choiyoi Group of southern Gondwana, in what is now South America, represents various Late Permian within-plate volcanics (McKay *et al*., 2016). U-Pb dating of the Choiyoi Group (Figure 18) constrains the Choiyoi Group to between 265 - 251 Ma and largely represents a trachyandesitic ash (Rocha-Campos *et al.,* 2011). Similarities in geochemistry, such as low Sr/Y (<40), Nb (10 - 35ppm), Y (70 - 90 ppm), and Zr (100 - 700ppm) between the Koppies deposit and Choiyoi Group are well established. Although this infers a distance of more than 1000 km from source to deposition (Viljoen, 1994), it is believed that this characteristic, and associated cooling of the ash, favoured the formation of the relatively high grade neoformed bentonite deposits. Similarly, Slaughter and Hamil (1970), analysed ash particle radii, palaeo winds and the sample distribution of various present-day ash and bentonite occurrences. The resultant calculations illustrated ash beds that ranged between 300 - 1000 km from the eruptive source further illustrating the atypical distances from source to deposition of tuffaceous material.

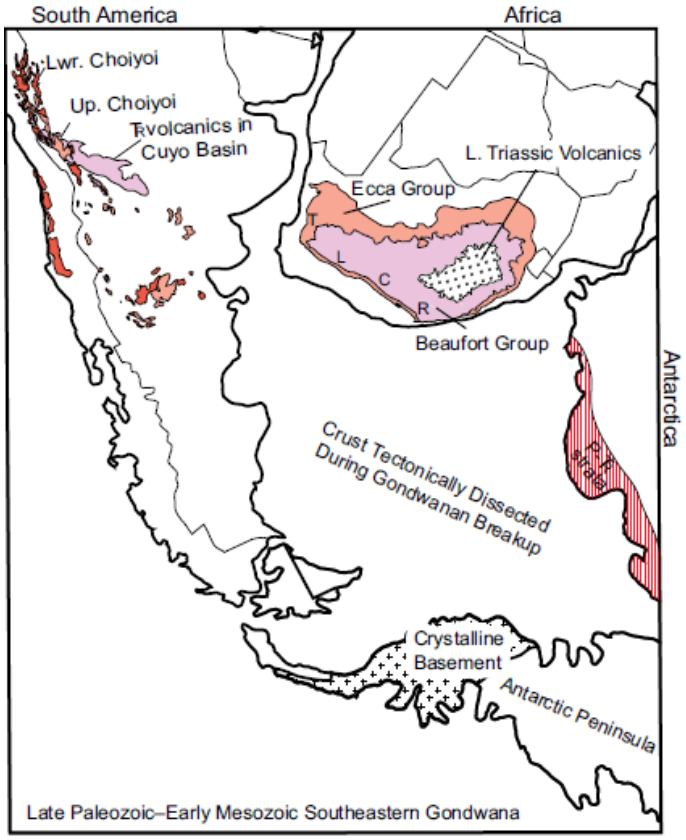


Figure 18: Simplified palaeo geological map illustrating the approximate distance between the Choiyoi Group and Volksrust Formation which is contained in the NW section of the Ecca Group (From: McKay *et al*., 2016).

6.3. Transport and deposition

Initial transport of trachyandesitic ash was likely to have been driven by aeolian processes comprising both high-altitude drift and dominant prevailing tropospheric winds which kept large quantities of ash particles in suspension over a large distance (Eaten, 1964). Upon ash fallout, the initial preservation of surficial particulates would have been deleterious to significant accumulation of ash particles as weathering processes would have eroded and redistributed the ash inefficiently (Berry, 1999). In contrast, the low energy environment of the MKB would have provided favourable conditions for ash to settle out of suspension and deposit on the floor of the laterally extensive basin (Slaughter and Hamil, 2013). Anomalous zircons point toward the input of detritus, albeit at a slower rate, contemporaneous with the deposition of precursor ash. However, similar process may have occurred near the margin of the basin or sub-basins (McKay *et al*., 2016). Further transport, evidenced by the rounded zircon crystals, was likely to have been driven by marine-dominated processes (convective flow) affected by contrasts in hydraulic gradient and permeability within the accumulated ash particles during cooling and diagenesis of the volcaniclastic material (Christidis, 2008).

Bentonite deposits derived from volcanic ash form as continuous stratigraphic horizons with sharp top and bottom contacts (Cabellero *et al*., 1992). Figure 19 illustrates an idealised setting for the deposition of the Koppies bentonite deposit, with the additional structural control of the Greenlands Formation to preserve the deposits. The modern topography is believed to mirror that of the palaeo-topography contemporaneous with the formation of the Koppies bentonite deposits (J.Horn, personal communication) based on coal exploration data obtained by Anglo American in the nearby vicinity. The combination of water transported along palaeo-lows, a low-energy environment and suitable embayments helped to preserve the ash deposits which were subsequently altered over geologic history.

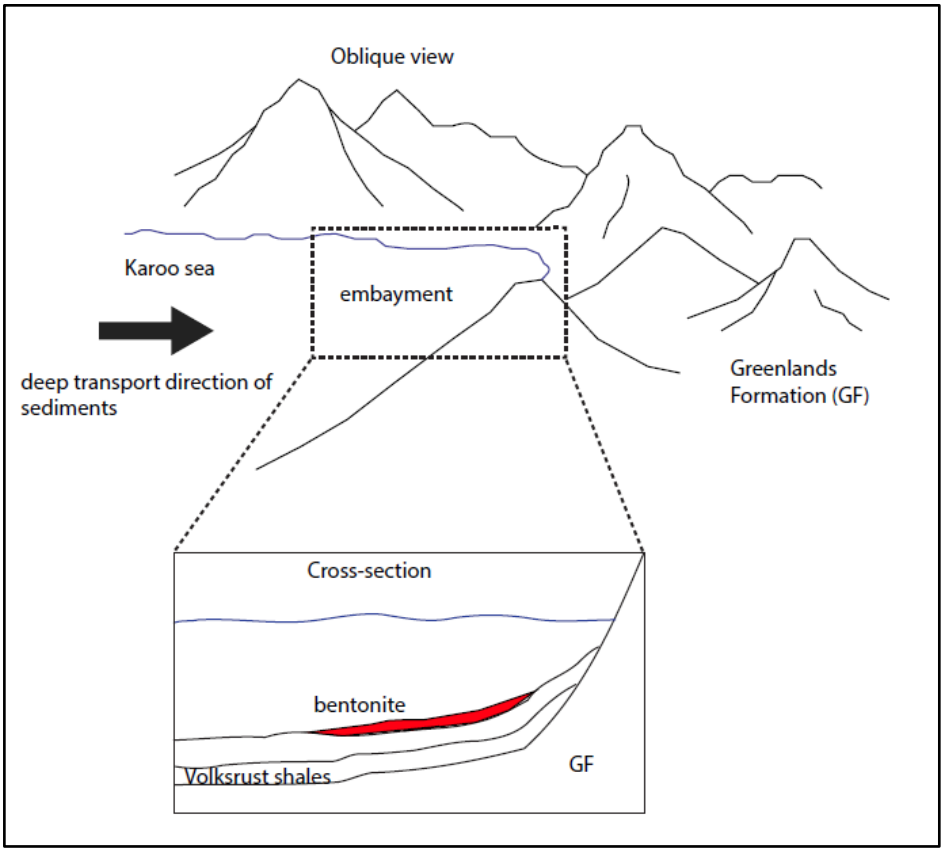


Figure 19: Idealised sketch of the depositional setting and the structural relationship between the Koppies bentonite and Greenlands Formation.

6.4. Alteration

Major and trace element geochemistry suggest an aerobic, alkaline (pH of 8.5), saline basin to promote bentonite formation. The orientation and geometry of the thick, stratiform orebody suggest a consistently low temperature differential between the pyroclastic ash and cooler surrounding water. Typically, elliptical orebodies are attributable to magmatic bodies and fracture zone interactions with less consistent temperature differentials (Christidis and Huff, 2009). Dissolution-precipitation occurred between the deposited ash, specifically the *in-situ*

glass constituent, and the saline water. This saline fluid (seawater) in the sedimentary basin was crucial for juvenile ash as it provided an additional source of Mg^{2+} to drive the reaction process (Horn and Strydom, 1998). A similar, modern-day Koppies-type bentonite would point towards a high temperature parent ash; however, the tuffaceous source material is established as a lower temperature parent glass, which was upgraded through a combination of diagenetic and supergene alteration processes to form the Koppies deposits.

Pervasive supergene weathering was promoted by a combination of saline water trapped within the sediments as the sea retreated and prolonged percolation of meteoric water after diagenesis - evidenced by a predominance of Mg^{2+}, Ca^{2+} cations, a smectite-dominated mineralogy and high Fe contents (Bazargani-Guilani *et al*., 2008). Silica nodules and concretions throughout the shallow extents of the orebody are attributed to secondary processes which occurred after alteration of the volcanic ash. Additionally, both organic and inorganic (carbonates, sulphates) materials were precipitated in joints or occur disseminated throughout the shallow restricted (sub-) basins due to high evaporitic and diagenetic conditions (Knechtel and Patterson, 1962). The characteristic stratigraphically continuous bentonite horizons with sharp top and bottom contacts which grade into surrounding smectite-rich shales are indicative of diagenesis. In summary, formation of magnesium and calcium rich di-octahedral smectite was promoted by an alkaline pH, abundance of basic cations, flat topography, high silica contents, poor drainage, a Mediterranean climate with wet and dry seasonal conditions and long-lived supergene processes.

6.5. Implications for exploration

As the Blaauwboschpoort and Oceaan bentonite deposits are related to a volcanic event and not the *in-situ* weathering of the acidic/alkaline Greenlands Formation, a relevant exploration model can be defined with the presumption that the pH, Eh, drainage, climate, stratigraphy and sedimentary conditions are similar for localised deposits. Consequently, exploration should ideally be focused along current drainage lines, which may have acted to transport precursor tuffaceous material and hence bentonite. Prospective areas include embayments around older, upturned geological units. Palaeo-lows, in conjunction with a shallow water table, would promote chemical alteration of a pre-cursor ash. Definition of a specific stratigraphic horizon within the Volksrust Formation for favourable bentonite formation is crucial in cost-saving and effective targeting for further (economical) deposits.

Chapter 7

Conclusion

The aim of this study was to define the source and processes responsible for the Koppies bentonite deposit and subsequently incorporate the results into a basic exploration model.

Initial field work illustrated that the Greenlands Formation did not weather *in-situ* to form bentonite, evidenced by the lack of allophane material, but rather acted as a structural palaeo-high. The palaeo-low embayments served as low energy environments for volcanic ash to deposit with further protection from physical weathering.

Chemical and mineralogical results indicate that the Koppies bentonite can be linked to an anorogenic 'within-plate granite setting', whereby voluminous, tuffaceous trachyandesitic ash were produced. Small, colourless zircon populations suggest a single ash source, with the presence of rare, large, rounded grains attributable to the input of externally sourced detritus during the depositional phase. A comparison between the geochemical signature of the Koppies bentonites and known Gondwanan events yielded a similarity between the Choiyoi Group volcanics located in South America, which is believed to have supplied the ash which led to the neoformation of the Koppies bentonite. Similarities including age (265 – 251 Ma), mineralogy, chemistry and location are strong supporting evidence. The lack of opal-CT within the bentonite also points to a lower thermal gradient between the water and tuffaceous ash which is the result of aeolian transport from a distant volcanic event. High-altitude drift and dominant prevailing tropospheric winds kept large quantities of ash particles in suspension over a great distance (>1000km). The low energy environment of the MKB would have provided favourable conditions for ash to settle out of suspension and deposit on the floor of the laterally extensive basin controlled by palaeo-lows lines and embayments.

The initial interaction of the seawater and subsequent meteoric water resulted in leaching of Si, K and Na and enrichment of Ca and Mg. Dissolution-precipitation between the glass constituent and water was subsequently followed by pervasive supergene weathering and diagenesis evidenced by a predominance of Mg^{2+}, Ca^{2+} cations, a smectite-dominated mineralogy, high Fe contents and a strong weathering pattern on the CIA graph.

The idealised targets for further bentonite exploration in the surrounding Volksrust Formation are low energy environments within palaeo-lows protected within embayments formed by upturned palaeo-lithologies that are much older than the Volksrust Formation. A defined

specific stratigraphic horizon within the Volksrust Formation for favourable bentonite formation is crucial in cost-saving and effective targeting of further economically-favourable deposits.

References

Al-Ani, T. and Sarapaa, O., 2008. Clay and clay mineralogy: physical-chemical properties and industrial uses. Geological survey of Finland, 30 June, pp. 1-91.

Altaner, S. P., Hower, J., Whitney, G. and Aronson, J. L., 1984. Model for K-bentonite formation: Evidence from zoned K-bentonites in disturbed belt, Montana. Geology, Volume 12(7), pp. 412-415.

Arslan, M., Abdioglu, E. and Kadir, S., 2010. Mineralogy, geochemistry, and the origin of bentonite in upper Cretaceous pyroclastic units of the Tirebolu area Giresun, northeast Turkey. Clay and clay minerals, Volume 58(1), pp. 120-141.

Bazargani-Guilani, K., Irajian, A.-A. and Youssefey, P., 2008. Geology and mineralogy of the bentonite deposits of the Kuh-e-Arshe, North Central Iran. Cambridge, IK, International Conference on Geology and Seismology.., pp. 94-99.

Berry, R., 1999. Eocene and oligocene Otay-type waxy bentonites of San Diego County and Baja California: chemistry, mineralogy, petrology and plate tectonic implications. clay and clay minerals, Volume 47, pp. 70-83.

Bhatia, M. and Crook, K., 1986. Trace element characteristics of graywackes and tectonic setting discrimination of sedimentary basins. Contributions to Mineralogy and Petrology, Volume 92, pp. 181-193.

Bordy, E. and Abrahams, M., 2016. Geochemistry of the Pronksberg Bentonite of the Upper Elliot Formation (Early Jurassic), Eastern Cape, South Africa. Origin and Evolution of the Cape Mountains and Karoo Basin, pp. 119-127.

Caballero, E. and Jimenez de Cisneros, C., 2017. Partitioning of minor, trace elements and rare earth elements in bentonite affecting by thermal alteration. Applied Clay Science, Volume 147, pp. 143-152.

Caballero, E., Reyes, E., Delgado, A., Huertas, F., and Linares, J.,1992. The formation of bentonite: mass balance effects. Applied Clay Science, Volume 6, pp. 265-276.

Caballero, E., Reyes, E., Huertas, F., Linares, J., and Pzzuoli, A., 1991. Early-stage smectites from pyroclastic rocks of Almeria (Spain). Chemical Geology, Volume 89, pp. 353-358.

Calarge, L., Meunier, A., Lanson, B. and Formoso, L., 2006. Chemical signiture of two permian volcanic ash deposits within a bentonite bed from Melo, Uruguay. Anais de Academia Brasileira de Ciencias, Volume 78(3), pp. 525-541.

Catuneanu, O., Hancox, P.J., Rubidge, B.S., 1998. Reciprocal flexural behaviour and contrasting stratigraphies: a new basin development model for the Karoo retroarc foreland system, South Africa. Basin Research, Volume 10, pp.417-439.

Catuneanu, O., Wopfner, H., Eriksson, P.G., Cairncross, B., Rubidge, B.S., Smith, R.M.H., and Hancox, P.J., 2005. The Karoo basins of south-central Africa. Journal of African Earth Sciences, Volume 43, pp. 211-253.

Christidis, G., 1998. Comparitive study of the mobility of major and trace elements during alteration of an andesite and a rhyolite to bentonite, in the islands of Milos and Kimolos, Aegean, Greece. Clay and clay minerals, Volume 46(4), pp. 379-399.

Christidis, G., 2001. Formation and growth of smectities in bentonites: a case study from Kimolos Island, Aegean, Greece. Clay and clay Minerals, Volume 49(3), pp. 204-215.

Christidis, G., 2008. Do bentonites have contradictory characteristics? An attempt to answer unanswered questions. Clay Minerals, Volume 43, pp. 515-529.

Christidis, G. and Huff, W., 2009. Geological aspects and genesis of bentonites. Elements, Volume 5(2), pp. 93-98.

Christidis, G., Scott, P. and Marcopoulos, T., 1995. Origin of the bentonite deposits of eastern Milos, Aegean, Greece: Geological, mineralogical and geochemical evidence. Clays and Clay Minerals, Volume 43, pp. 63-77.

Coetzee, C. and Hanekom, H., 1966. Note on the bentonite in the Parys area.

Corfu, F., Hanchar, J., Hoskin, P. and Kinny, P., 2003. Atlas of Zircon Textures. Zircon, Volume 53(1), pp. 469-495.

Dill, H., 2010. The "chessboard" classification scheme of mineral deposits: Mineralogy and geology from aluminium to zirconium. Earth-Science Reviews, Volume 100(1-4), pp. 1-420.

Dill, H., 2017. Residual clay deposits in basement rocks: The impact of climate and the geological setting on supergene argillitization in the Bohemian Massif (Central Europe) and across the globe. Earth-Science Reviews, Volume 165, pp. 1-58.

dos Muchangos, A. C., 2006. The mobility of rare-earth and other elements in the process of alteration of rhyolitic rocks to bentonite (Lebombo Volcanic Mountainous Chain, Mozambique). Journal of Geochemical Exploration, Volume 88(1-3), pp. 300-303.

Dypvik, H. and Harris, N., 2001. Geochemical facies analysis of fine-grained siliciclastics using Th/ U, Zr/ Rb and (Zr+Rb)/ Sr ratios. Chemical Geology, Volume 181, pp. 131-146.

Eaton, G., 1964. Windborne volcanic ash: A possible index to polar wandering. The Journal of Geology, Volume 72(1), pp. 1-35.

Elzea, J. and Murray, H., 1990. Variation in the mineralogical, chemical and physical properties of the Cretaceous Clay Spur bentonite in Wyoming and Montana (U.S.A.). Applied Clay Science, Volume 5(3), pp. 229-248.

Enslin, F., van der Mey, L. and Waanders, F., 2010. Acid leaching of heavy metals from bentonite clay, used in the cleaning of acid mine drainage. The Journal of the South African Institute of Mining and Metallurgy, Volume 110, pp. 187-191.

Galan, E., 2006. Genesis of clay minerals. In: F. Bergaya, B. Theng & G. Lagaly, eds. Handbook of clay science. Elsevier Limited, pp. 1129-1162.

Gardam, M., Mason, A.J., Reid, A.F., Churchman, G.J., and Raven, M., 2009. Arumpo bentonite deposits: distinctive indicators of past volcanic events in the Murray Basin, southeastern Australia. Australian Journal of Earth Science: An International Geoscience Journal of the Geological Society of Australia, Volume 55(2), pp. 183-194.

Geel, C., Schulz, H-M., Booth, P., deWit, M., Horsfield, B., 2013. Shale Gas Characteristics of Permain Black Shales in South Africa: Results from Recent Drilling in the Ecca Group (Eastern Cape), Energy Procedia, Volume 40, pp.256-265.

Goldich, S. S., 1938. A study in rock weathering. The Journal of Geology, Volume 46(1), pp. 17-58.

Gong, Z., Liao, L., Lv, G. and Wang, X., 2016. A simple method for physical purification of bentonite. Applied Clay Science, Volume 119, pp. 294-300.

Grim, R., 1972. Technical properties and applications of clays and clay minerals. Madrid, Haverly, Belgium: Association International pour l'Etude des Argiles (AIPEA), pp. 719-721.

Grim, R. and Guven, N., 1978. Developments in Sedimentology: Bentonites, Elsevier Science.

Hancox, P.J., Gotz, A.E., 2014. South Africa's coalfields - A 2014 perspective, International Journal of Coal Geology, Volume 132, pp. 170-254

Heckroodt, R., 1991. Clay and clay minerals in South Africa. Journal of South African Institute of Mining and Metallurgy, Volume 91(10), pp. 343-363.

Henderson, J., Jackson, M.L., Syers, J.K.., Clayton, R.N., and Rex, R.W., 1971. Cristobalite authigenic origin in relation to montmorillonite and quartz origin in bentonites. Clays and clay minerals, Volume 19, pp. 229-238.

Horn, G. and Strydom, J., 1998. Clay: The Mineral Resources of South Africa. Pretoria: Council for Geoscience.

Huff, W., 2008. Ordovician K-bentonites: Issues in interpreting and correlating ancient tephras. Quaternary International, Volume 178, pp. 276-287.

Huff, W., Bergstrom, S., Kolata, D. and Sun, H., 1998. The lower Silurian Osmundsberg K-bentonite. Part II: mineralogy, geochemistry, chemostratigraphy and tectonomagnetic significance. The Geological Magazine, Volume 135(1), pp. 15-26.

Hunter, D., Johnson, M., Anhaeusser, C. and Thomas, R., 2006. Introduction. In: The Geology of South Africa. Pretoria, Johannesburg, South Africa: Geological Society of South Africa, Council for Geoscience.

Johnson, M., van Vuuren, C.J., Hegenberger, W.F., Key, R., and Shoko, U., 1996. Stratigraphy of the Karoo Supergroup in southern Africa: an overview. Journal of African Sciences, Volume 23(1), pp. 3-15.

Johnson, M., van Vuuren, C.J., Visser, J.N.J., Cole, D.I., de V. Wickens, H., Christie, A.D.M., Roberts, D.L., and Brandl, G., 2006. Sedimentary rocks of the Karoo Supergroup. In: The Geology of South Africa. Pretoria: Geological Society of South Africa, Council for Geoscience.

Keyser, N. and Zawanda, P., 1988. Two occurances of ash-flow tuff from the lower Beaufort Group in the Heilbron-Frankfort area, northern Orange Free State. South African Journal of Geology, Volume 91, pp. 509-521.

Knechtel, M. and Patterson, S., 1962. Bentonite deposits of the northern black hills district, Wyoming, Montana and South Dakota. Contributions to economic geology, pp. 803-1029.

Lana, C., Gibson, R. and Reimold, W., 2006. The Broodkop shear zone, southeast Vredefort dome (South Africa): A Dominion-related extensional feature? South African Journal of Geology, Volume 109(3), pp. 265-278.

Lana, C., Gibson, R., Reimold, W. and Minnitt, R., 2003. Geology and geochemistry of a granite-greenstone association in the south eastern Vredefort dome, South Africa. South African Journal of Geology, Volume 106(4), pp. 291-314.

Manninen, T., Eerola, T., Makitie, H., Vuori, S., Luttinen, A., Senvano, A., and Manhica, V., 2008. The Karoo volcanic rocks and related intrusions in southern and central Mozambique. Geological Survey of Finland, Volume 48, pp. 211-250.

McKay, M., Coble, M.A., Hessler, A.M., Weislogel, A.L., Fildani, A., 2016. Petrogenesis and provenance of distal volcanic tuffs from the Permian-Triassic Karoo Basin, South Africa: A window into a dissected magmatic province. Geosphere, Volume 12(1), pp. 1-14.

McLachlan, I. and Jonker, J., 1990. Tuff beds in the north western part of the Karoo Basin. South African Journal of Geology, Volume 93, pp. 329-338.

Minnitt, R. and Reimold, W., 2000. Greenlands Formation. Catalogue of South African lithostratigraphic units, Council for Geoscience, Pretoria, South Africa, Volume 6, pp. 6.5-6.6.

Minnitt, R., Reimold, W. and Colliston, W., 1994. The geology of the Greenlands Greenstone Complex and selected granitoid terranes in the south-eastern quadrant of the Vredefort Dome. Economic Geology Research Unit Information Circular, University of Witwatersrand, Johannesburg, South Africa, Volume 281, p. 46.

Murray, H., 2007. Applied Clay Mineralogy. Oxford, UK: Elsevier.

Pearce, J.A., Harris, N.B., and Tindle, A.G., 1984. Trace element discrimination diagrams for the tectonic interpretation of granitic rocks. Journal of Petrology, Volume 25, pp. 956-983

Pellenard, P., Deconinck, J-F., Huff, W.D., Thierry, J., Marchand, D., Fortwenglers, D., and Trouiller, A., 2003. Characterization and correlation of Upper Jurassic (Oxfordian) bentonite deposits in the Paris Basin and the Subalpine Basin, France. Sedimentology, Volume 50, pp. 1035-1060.

Puspoki, Z., Kozak, M., Kovacs-Palffy, P., Foldvari, M., McIntosh, R.W., and Vincze, L., 2005. Eustatic and tectonic/volcanic control in sedimentary bentonite formation- A case study of Miocene bentonite deposits from the Pannanian Basin. Clay and Clay Minerals, Volume 53(1), pp. 71-91.

Reimold, W. and Gibson, R., 1996. Geology and evolution of the Vredefort Impact Structure. South Africa. Journal of African Earth Science, Volume 23(2), pp. 125-162.

Reimold, W., Pybus, G.Q.J., Kruger, F.J., Layer, P.W., and Koeberl, C., 2000. The Anna's Rust Sheet and related gabbroic intrusions in the Vredefort Dome-Kibaran magmatic event on the Kaapvaal Craton and beyond? Journal of African Earth Sciences, Volume 31, pp. 499-521.

Rocha-Campos, A., Basei, M.A.S., Nutman, A.P., Kleiman, L.E., Varela, R., Llambias, E., Canile, F.M., da Rosa, O., de, C.R., 2011. 30 million years of Permian volcanism recorded in the Choiyoi igneous province (W Argentina) and their source for younger ash fall deposits in the Parana Basin: SHRIMP U-Pb zircon geochronology evidence. Gondwana Research, Volume 19, pp. 509-523.

Ross, C. and Shannon, E., 1926. Minerals of bentonite and related clays and their physical properties. Journal of American Ceramic Society, Volume 9, pp. 77-96.

Schmidt, E., 1976. In: Clay in Mineral Resources of South Africa: Handbook. Pretoria: Geological Survey of South Africa, pp. 299-311.

Scogings, A., 2016. Soaking it up: Bentonites global reach. Industrial Minerals Magazine, June, pp. 37-42.

Sircombe, K. and Stern, R. A., 2002. An investigation of artificial biasing in detrital zircon U-Pb geochronology due to magnetic separation in sample preparation. Geochemica et Cosmochimica Acta, Volume 66, pp. 2379-2397.

Slaughter, M. and Hamil, M., 2013. Model for deposition of volcanic ash and resulting bentonite, Geological society of America.

Slawson, W., 1976. Vredefort core: a cross section of the upper crust. Geochemica et Cosmochima Acta, Volume 40, pp. 117-121.

Smith, D., 1967. The petrology and mineralogy of some lower Devonian bentonites from Gaspe, P.Q. The Canadian Mineralogist, Volume 9, pp. 141-165.

Smith, R., Eriksson, P. and Botha, W., 1993. A review of the stratigraphy and sedimentary environments of the Karoo-aged basins of Southern Africa. Journal of African Earth Sciences, Volume 16, pp. 143-169.

Takagi, T., Koh, S.M., Song, M.S., Itoh, M., and Mogi, K., 2016. Geology and properties of the Kawasaki and Dobuyama bentonite deposits of Zao region in northwest Japan. Clay Minerals, Volume 40(3), pp. 333-350.

Thorson, T., 1997. Aerial surveying of Wyoming bentonite. Applied Clay Science, Volume 11, pp. 329-335.

Tucker, R. Roberts, E.M., Hu, Y., Kemp, A.I.S., 2013. Detrital zircon age constraints for the Winton Formation, Queensland: Contextualizing Australia's Late Cretaceous dinosaur faunas. Gondwana Research, Volume 24, pp. 767-779.

Viljoen, J., 1994. Sedimentology of the Collingham Formation, Karoo Supergroup. South African Journal of Geology, Volume 97, pp. 167-183.

Weltie, G. and von Eynatten, H., 2004. Quantitative provenance analysis of sediments: review and outlook. Sedimentary Geology, Volume 171, pp. 1-11.

Winchester, J.A. and Floyd, P.A., 1977. Geochemical discrimination of different magma series and their differentiation products using immobile elements. Chemical Geology, Volume 20, pp. 325-343.